Intrinsic Benefits of Categorical Distributional Loss: Uncertainty-aware Regularized Exploration in Reinforcement Learning

Ke Sun¹ Yingnan Zhao² Enze Shi¹ Yafei Wang¹ Xiaodong Yan³ Bei Jiang¹ Linglong Kong¹

Abstract

The remarkable empirical performance of distributional reinforcement learning (RL) has garnered increasing attention to understanding its theoretical advantages over classical RL. By decomposing the categorical distributional loss commonly employed in distributional RL, we find that the potential superiority of distributional RL can be attributed to a derived distribution-matching entropy regularization. This less-studied entropy regularization aims to capture additional knowledge of return distribution beyond only its expectation, contributing to an augmented reward signal in policy optimization. In contrast to the vanilla entropy regularization in MaxEnt RL, which explicitly encourages exploration by promoting diverse actions, the novel entropy regularization derived from categorical distributional loss implicitly updates policies to align the learned policy with (estimated) environmental uncertainty. Finally, extensive experiments substantiate the significance of this uncertainty-aware regularization from distributional RL on the empirical benefits over classical RL. Our study offers a new perspective from the exploration to explain the intrinsic benefits of adopting distributional learning in RL.

1. Introduction

The fundamental characteristics of classical reinforcement learning (RL) (Sutton & Barto, 2018), such as Q-learning (Watkins & Dayan, 1992), rely on estimating the expectation of discounted cumulative rewards that an agent observes while interacting with the environment. In contrast to the expectation-based RL, a novel branch of algorithms, termed *distributional RL*, seeks to estimate the entire distri-

Preprint.

bution of total returns and has achieved state-of-the-art performance across a diverse array of environments (Bellemare et al., 2017a; Dabney et al., 2018b;a; Yang et al., 2019; Zhou et al., 2020; Nguyen et al., 2020; Wenliang et al., 2024; Sun et al., 2024b; Rowland et al., 2024b). Meanwhile, discussions of distributional RL have increasingly extended into a wider range of fields, such as risk-sensitive control (Dabney et al., 2018a; Lim & Malik, 2022; Chen et al., 2024), offline learning (Ma et al., 2021; Wu et al., 2023), policy exploration (Mavrin et al., 2019; Rowland et al., 2019; Cho et al., 2023), robustness (Sun et al., 2023; Sui et al., 2023; Rowland et al., 2023), optimization (Rowland et al., 2023; Kuang et al., 2023; Sun et al., 2024a), statistical inference (Zhang et al., 2023), multivariate rewards (Zhang et al., 2021; Wiltzer et al., 2024b), and continuous-time setting (Wiltzer et al., 2024a).

Motivation: Understanding the Benefits of Employing (Categorical) Distributional Loss in RL. Despite the impressive empirical success of distributional RL algorithms, our comprehension of their advantages over classical RL remains incomplete, especially for the general function approximation setting and practical implementations. Early work (Lyle et al., 2019) demonstrated that in many realizations of tabular and linear approximation settings, distributional RL behaves similarly to classic RL, suggesting that its benefits are mainly realized in the non-linear approximation setting. Although their findings offer profound insights, their analysis, based on a coupled update method, overlooks several factors, such as the optimization effect under various losses. The statistical benefits of quantile temporal difference (QTD), employed in quantile distributional RL, e.g., QR-DQN (Dabney et al., 2018b), were highlighted in (Rowland et al., 2023; 2024a), which posited that the robust estimation of QTD fosters the benefits in stochastic environments. The foundational theoretical aspects of Categorical Distributional RL (CDRL), e.g., C51 (Bellemare et al., 2017a), were first discussed in (Rowland et al., 2018); however, explaining the advantages of categorical distributional learning remains under-explored. Furthermore, recent studies (Wang et al., 2023; 2024) elucidate the benefits of distributional RL by introducing the small-loss and secondorder PAC bounds, revealing the enhanced sample efficiency, particularly in specific cases with small achievable costs.

¹Department of Mathematical and Statistical Sciences, University of Alberta ²Department of Computer Science and Technology, Harbin Engineering University ³Zhongtai Securities Institute for Financial Studies, Shangdong University. Correspondence to: Linglong Kong < lkong@ualberta.ca>.

Yet, their findings are not directly based on practical distributional RL algorithms, such as C51 or QR-DQN. Therefore, it is imperative to close this gap between understanding their theoretical advantages and practical deployment in complex environments for distributional RL algorithms.

Contributions. In this study, we interpret the potential superiority of distributional learning in RL over classical RL, specifically focusing on CDRL, the pioneering family within distributional RL. We examine the benefits through the lens of a regularized exploration effect, offering a distinct perspective relative to existing literature. Our investigation begins by decomposing the categorical distributional loss into a mean-related term and a distribution-matching regularization term, facilitated by our proposed return density decomposition technique. The resulting regularization acts as an augmented reward in the actor critic framework, encouraging policies to explore states whose current return distribution estimates lag far behind the (estimated) environmental uncertainty in the target return. This derived regularization from the categorical distributional loss in CDRL promotes an uncertainty-aware exploration effect, which diverges from the exploration for diverse actions commonly used in MaxEnt RL (Williams & Peng, 1991; Haarnoja et al., 2018a;b). We also provide the convergence foundations when leveraging the decomposed uncertain-aware regularization in the actor critic. Empirical evidence underscores the pivotal role of the uncertainty-aware entropy regularization in the empirical success of adopting categorical distributional loss in RL over classical RL on both Atari games and MuJoCo tasks. We further elucidate the distinct roles that the uncertainty-aware entropy in distributional RL and the vanilla entropy in MaxEnt RL play by exploring their mutual impacts on learning performance. This opens new avenues for future research in this domain. Our contributions are summarized as follows:

- 1. By applying a return density decomposition on the categorical distributional loss, we derive a distribution-matching regularization. This regularization promotes uncertainty-aware exploration, interpreting the benefits of categorical distributional learning in RL.
- In the actor critic, we further compare the different exploration effects of our decomposed uncertainty-aware regularization from distributional RL and the vanilla entropy regularization in MaxEnt RL.
- 3. Empirically, we verify the uncertainty-aware regularization effect on the performance advantage of distributional RL over classical RL and explore the mutual impacts of two types of regularization in learning.

Outline. We provide the related work and background knowledge in Sections 2 and 3, respectively. We begin by

interpreting the benefits of categorical distributional learning as uncertainty-aware regularized exploration in *value-based* RL in Section 4. We further probe this exploration benefit *in the actor critic* in Section 5, where we directly compare it with the vanilla entropy regularization in MaxEnt RL. Extensive experiments demonstrate the benefits of regularized exploration in distributional RL and its mutual impact with entropy regularization in MaxEnt RL in Section 6.

2. Related Work

Distributional Learning via Categorical Representation.

Categorical learning has been widely employed, with advantages in representation (Pan et al., 2019; Jang et al., 2016) and optimization (Imani & White, 2018; Sun et al., 2024a). Recently, the empirical superiority of categorical distribution learning has been further investigated in various RL tasks (Farebrother et al., 2024). Thus, a pressing need exists to examine the theoretical foundations of categorical distributional learning, particularly in RL. The perspective of uncertainty-aware regularized exploration our study introduces provides significant insights into understanding the benefits of being categorical distributional in RL.

Uncertainty-oriented Exploration. Uncertainty-oriented exploration plays an integral part in existing exploration methods (Hao et al., 2023), which leverages uncertainty either in the (posterior) estimation of the value function, as seen in Bayesian framework (Osband et al., 2016b; Azizzadenesheli et al., 2018), Bootstrap (Osband et al., 2016a), and Ensemble methods (Lee et al., 2021), or in the entire distribution of returns (Tang & Agrawal, 2018; Mavrin et al., 2019; Cho et al., 2023). For example, Decaying Left Truncated Variance (DLTV) (Mavrin et al., 2019) and Perturbed Quantile Regression (PQR) (Cho et al., 2023) exploits the variability of the learned return distribution to promote an optimistic exploration in distributional RL. In contrast, the primary aim of this study is to demonstrate that distributional learning in RL entails an intrinsic exploration effect against environmental uncertainty, contributing to the outperformance of distributional RL over classical RL. Our study goal is independent of designing advanced exploration strategies on top of distributional RL. Similarly, MaxEnt RL (Williams & Peng, 1991), which includes soft Q-learning (Haarnoja et al., 2017), Soft Actor Critic (SAC) (Haarnoja et al., 2018a) and their variants (Han & Sung, 2021), also promotes uncertainty-oriented exploration by relying on the stochasticity of the learned policy. A more detailed discussion is provided in Appendix A.

3. Preliminaries

Markov Decision Process (MDP) and Classical RL. An environment is modeled via an Markov Decision Pro-

cess $(\mathcal{S},\mathcal{A},\mathcal{R},P,\gamma)$, with a set of states \mathcal{S} and actions \mathcal{A} , the bounded reward function $\mathcal{R}:\mathcal{S}\times\mathcal{A}\to\mathcal{P}([R_{\min},R_{\max}])$, the transition kernel $P:\mathcal{S}\times\mathcal{A}\to\mathcal{P}(\mathcal{S})$, and a discounted factor $\gamma\in[0,1]$. We denote the reward the agent receives at time t as $r_t\sim\mathcal{R}(s_t,a_t)$. Given a policy π , the key quantity of interest is the return Z^π , which is the total cumulative rewards over the course of a trajectory defined by $Z^\pi(s,a)=\sum_{t=0}^\infty \gamma^t r_t|s_0=s, a_0=a$. Classical RL focuses on estimating the expectation of the return, i.e., $Q^\pi(s,a)=\mathbb{E}_\pi\left[\sum_{t=0}^{+\infty} \gamma^t r_t|s_0=s, a_0=a\right]$. We also define Bellman evaluation operator $\mathcal{T}^\pi Q(s,a)=\mathbb{E}[\mathcal{R}(s,a)]+\gamma\mathbb{E}_{s'\sim P,a'\sim\pi}\left[Q\left(s',a'\right)\right]$, and Bellman optimality operator $\mathcal{T}^{\text{opt}}Q(s,a)=\mathbb{E}[\mathcal{R}(s,a)]+\gamma\max_{a'}\mathbb{E}_{s'\sim P}\left[Q\left(s',a'\right)\right]$.

Distributional RL and CDRL. Instead of only learning the expectation in classical RL, distributional RL models the full distribution of the return Z^{π} . The return distribution $\eta^{\pi}: \mathcal{S} \times \mathcal{A} \to \mathcal{P}(\mathbb{R})$ is defined as $\eta^{\pi}(s, a) = \mathcal{D}(Z^{\pi}(s, a))$, where \mathcal{D} extracts the distribution of a random variable. $\eta^{\pi}(s,a)$ is updated via the distributional Bellman operator \mathfrak{T}^{π} , defined by $\mathfrak{T}^{\pi}Z(s,a) \stackrel{D}{=} \mathcal{R}(s,a) + \gamma Z(s',a')$, where $\stackrel{D}{=}$ implies that random variables of both sides are equal in distribution. Categorical Distributional RL (CDRL) (Bellemare et al., 2017a), e.g., C51, is the first successful distributional RL family that approximates the return distribution by a discrete categorical distribution $\widehat{\eta}^{\pi} = \sum_{i=1}^{N} p_i \delta_{z_i}$, where $\{z_i\}_{i=1}^{N}$ is a set of fixed supports and $\{p_i\}_{i=1}^{N}$ are learnable probabilities. The leverage of a heuristic projection operator $\Pi_{\mathcal{C}}$ (see Appendix B for more details) and the Kullback-Leibler (KL) divergence guarantee the theoretical convergence of CDRL under Cramér distance or Wasserstein distance in the tabular setting (Rowland et al., 2018).

4. Regularization Benefits in Value-based Distribution RL

In this section, we simplify value-based distributional RL to a Neural Fitted Z-Iteration (Neural FZI) process in Section 4.1, within which the distributional loss used in distributional RL can be further rewritten as an entropy-regularized form as shown in Section 4.2. Finally, we characterize the role of the derived entropy-based regularization as uncertainaware regularized exploration in Section 4.3.

4.1. Distributional RL: Neural FZI

Classical RL: Neural Fitted Q-Iteration (Neural FQI). Neural FQI (Fan et al., 2020; Riedmiller, 2005) offers a statistical explanation of DQN (Mnih et al., 2015), capturing its key features, including experience replay and the target network Q_{θ^*} . In Neural FQI, we update a parameterized Q_{θ} in each iteration k of an iterative regression framework: $Q_{\theta}^{k+1} = \operatorname{argmin}_{Q_{\theta}} \frac{1}{n} \sum_{i=1}^{n} \left[y_i^k - Q_{\theta} \left(s_i, a_i \right) \right]^2$ (Neural FQI), where the target $y_i^k = r(s_i, a_i)$

 $\gamma \max_{a \in \mathcal{A}} Q_{\theta^*}^k (s_i', a)$ is fixed within every T_{target} steps to update target network Q_{θ^*} by letting $Q_{\theta^*}^k = Q_{\theta}^k$. The experience buffer induces independent samples $\{(s_i, a_i, r_i, s_i')\}_{i \in [n]}$. If $\{Q_{\theta} : \theta \in \Theta\}$ is sufficiently large such that it contains $\mathcal{T}^{\text{opt}}Q_{\theta^*}^k$, i.e., the realizable assumption in learning theory (Mohri, 2018), Neural FQI has the solution $Q_{\theta}^{k+1} = \mathcal{T}^{\text{opt}}Q_{\theta^*}^k$, which is exactly the updating rule under Bellman optimality operator (Fan et al., 2020).

Distributional RL: Neural Fitted Z-Iteration (Neural FZI). Analogous to Neural FQI, we simplify value-based distributional RL algorithms with the parameterized Z_{θ} into Neural FZI, which is formulated as

$$Z_{\theta}^{k+1} = \underset{Z_{\theta}}{\operatorname{argmin}} \frac{1}{n} \sum_{i=1}^{n} d_{p}(Y_{i}^{k}, Z_{\theta}(s_{i}, a_{i})), \qquad (1)$$

where we denote the target return as $Y_i^k = \mathcal{R}(s_i, a_i) + \gamma Z_{\theta^*}^k (s_i', \pi_Z(s_i'))$ with the policy π_Z following the greedy rule $\pi_Z(s_i') = \operatorname{argmax}_{a'} \mathbb{E}\left[Z_{\theta^*}^k(s_i', a')\right]$. The target Y_i^k is fixed within every T_{target} steps to update target network Z_{θ^*} . d_p is a distribution divergence between two distributions. While our analysis is not intended to involve properties of deep neural networks, we interpret distributional RL as Neural FZI as it is by far closest to the practical algorithms.

4.2. Distributional RL: Entropy-regularized Neural FQI

As mentioned previously in preliminary knowledge (Section 3), CDRL employs neural networks to learn the probabilities $\{p_i\}_{i=1}^N$ in a discrete categorical distribution to represent Z_θ , and choose KL divergence as d_p in Eq. 1 of Neural FZI. We next decompose the KL-based distributional loss d_p in CDRL by utilizing an equivalent histogram density estimator \widehat{p} in representing Z_θ .

Return Density Decomposition. To characterize the impact of additional knowledge from the return distribution beyond its expectation, we use a variant of gross error model from robust statistics (Huber, 2004), which was also similarly applied to analyze Label Smoothing (Müller et al., 2019) and Knowledge Distillation (Hinton et al., 2015). Akin to the categorical parameterization in CDRL, we utilize a histogram function estimator $\widehat{p}^{s,a}(x)$ with N bins to approximate an arbitrary continuous density $p^{s,a}(x)$ of $Z^{\pi}(s,a)$, given a state s and action a. In contrast to categorical parameterization defined on a set of fixed supports, the histogram estimator operates over a continuous interval, enabling more nuanced analysis within continuous functions. Given a fixed set of supports $l_0 \leq l_1 \leq ... \leq l_N$ with the equal bin size as Δ , each bin is thus denoted as $\Delta_i = [l_{i-1}, l_i), i = 1, ..., N-1 \text{ with } \Delta_N = [l_{N-1}, l_N].$ As such, the histogram density estimator is formulated by $\widehat{p}^{s,a}(x) = \sum_{i=1}^N p_i \mathbb{1}(x \in \Delta_i)/\Delta$ with p_i as the coefficient in the *i*-th bin Δ_i . Denote Δ_E as the interval that $\mathbb{E}[Z^{\pi}(s,a)]$ falls into, i.e., $\mathbb{E}[Z^{\pi}(s,a)] \in \Delta_E$. Putting all

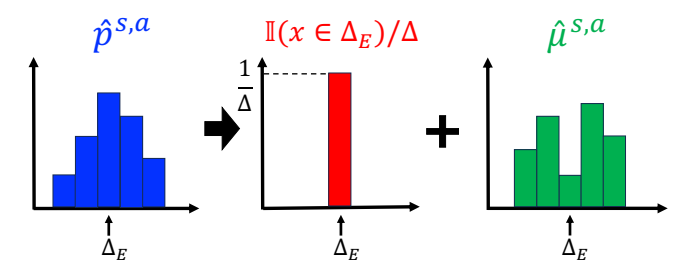


Figure 1: Return Density Decomposition on Histograms.

together, we apply an action-state return density decomposition over the histogram density estimator $\hat{p}^{s,a}$:

$$\widehat{p}^{s,a}(x) = (1 - \epsilon) \mathbb{1}(x \in \Delta_E) / \Delta + \epsilon \widehat{\mu}^{s,a}(x), \quad (2)$$

where $\widehat{p}^{s,a}$ is decomposed into a single-bin histogram $\mathbb{1}(x \in$ $(\Delta_E)/\Delta$ with all mass on (Δ_E) and an **induced** histogram density function $\widehat{\mu}^{s,a}$ evaluated by $\widehat{\mu}^{s,a}(x) = \sum_{i=1}^N p_i^\mu \mathbb{1}(x \in \Delta_i)/\Delta$ with p_i^μ as the coefficient of the *i*-th bin Δ_i . is a hyper-parameter pre-specified before the decomposition, controlling the proportion between $\mathbb{1}(x \in \Delta_E)/\Delta$ and $\widehat{\mu}^{s,a}(x)$. See Figure 1 for the illustration of the decomposition. More specifically, the induced histogram density function $\widehat{\mu}^{s,a}$ in the second term of Eq. 2 represents the difference between the full histogram function $\hat{p}^{s,a}$ and a single-bin histogram $\mathbb{1}(x \in \Delta_E)/\Delta$, where $\mathbb{1}(x \in \Delta_E)/\Delta$ only captures the mean. This difference indicates that $\widehat{\mu}^{s,a}$ captures the additional distribution information of $Z^{\pi}(s,a)$ beyond its expectation $\mathbb{E}[Z^{\pi}(s,a)]$, incorporating highermoments information. This reflects the influence of using a full distribution on the performance of distributional RL. The additional leverage of $\hat{\mu}^{s,a}$ in the distributional loss explains the behavior differences between classical and distribution RL algorithms. We next demonstrate that $\widehat{\mu}^{s,a}$ is a valid probability density under certain ϵ in Proposition 1.

Proposition 1. (Decomposition Validity) Denote $\widehat{p}^{s,a}(x \in \Delta_E) = p_E/\Delta$, where p_E is the coefficient on the bin Δ_E . $\widehat{\mu}^{s,a}(x) = \sum_{i=1}^N p_i^\mu \mathbb{1}(x \in \Delta_i)/\Delta$ is a valid density if and only if $\epsilon \geq 1 - p_E$.

The proof can be found in Appendix C. Proposition 1 demonstrates that the return density decomposition is valid when the hyper-parameter ϵ is well specified as $\epsilon \geq 1-p_E$. Under this condition, our analysis maintains the standard categorical distributional learning in distributional RL.

Equivalence between Histogram Parameterization and Categorical Representation. The histogram function is a continuous estimator in contrast to the discrete nature of categorical parameterization. Although relatively straightforward, we demonstrate their equivalence in representing a density function in Appendix D. As a supplementary analysis, with attribution to (Wasserman, 2006), we also discuss

necessary theoretical underpinnings of the histogram density estimator in the context of distributional RL in Appendix E.

Distributional RL: Entropy-regularized Neural FQI. We apply the decomposition in Eq. 2 on the histogram density function, denoted as $\widehat{p}^{s'_i,\pi_Z(s'_i)}$, of the target return $Y^k_i=\mathcal{R}(s_i,a_i)+\gamma Z^k_{\theta^*}$ $(s'_i,\pi_Z(s'_i))$ in Eq. 1 of Neural FZI. Consequently, we have $\widehat{p}^{s'_i,\pi_Z(s'_i)}(x)=(1-\epsilon)\mathbb{1}(x\in\Delta^i_E)/\Delta+\epsilon\widehat{\mu}^{s'_i,\pi_Z(s'_i)}(x)$, where Δ^i_E represents the interval that the expectation of the target return Y^k_i falls into, i.e., $\mathbb{E}\left[Y^k_i\right]\in\Delta^i_E$, and $\widehat{\mu}^{s'_i,\pi_Z(s'_i)}$ is the induced histogram density function, similar to the role of $\widehat{\mu}^{s,a}$ in Eq. 2. Let $\mathcal{H}(U,V)$ be the cross-entropy between two probability measures U and V, i.e., $\mathcal{H}(U,V)=-\int_{x\in\mathcal{X}}U(x)\log V(x)\,\mathrm{d}x$. Immediately, we can derive the following entropy-regularized loss function form of Neural FZI for distributional RL in Proposition 2. The proof is provided in Appendix G.

Proposition 2. (Decomposed Neural FZI) Denote $q_{\theta}^{s,a}$ as the histogram density estimator of $Z_{\theta}^{k}(s,a)$ in Neural FZI. Based on the decomposition in Eq. 2 and the KL divergence as d_{v} , the Neural FZI process in Eq. 1 is simplified as

$$Z_{\theta}^{k+1} = \underset{q_{\theta}}{\operatorname{argmin}} \frac{1}{n} \sum_{i=1}^{n} \underbrace{\left[-\log q_{\theta}^{s_{i}, a_{i}}(\Delta_{E}^{i})\right]}_{Mean-Related\ Term} + \underbrace{\alpha \mathcal{H}(\widehat{\mu}^{s_{i}', \pi_{Z}(s_{i}')}, q_{\theta}^{s_{i}, a_{i}})\right]}_{Recularization\ Term},$$
(3)

where $\alpha = \varepsilon/(1-\varepsilon) > 0$ and the mean-related term is negative log-likelihood function centered on Δ_E^i .

Connection between Neural FQI and FZI. A crucial bridge between classical and distributional RL is established in Proposition 3, where we demonstrate that minimizing the mean-related term in Eq. 3 of Neural FZI is asymptotically equivalent to minimizing Neural FQI in terms of the minimizers as $\Delta \to 0$. As such, the regularization term $\alpha \mathcal{H}(\widehat{\mu}^{s'_i,\pi_Z(s'_i)},q^{s_i,a_i}_{\theta})$ interprets the potential benefits of CDRL over classical RL. For the uniformity of notation, we still use s,a in the following analysis instead of s_i,a_i .

Proposition 3. (Equivalence between the Mean-Related term in Decomposed Neural FZI and Neural FQI) In Eq. 3, assume the function class $\{Z_{\theta}: \theta \in \Theta\}$ is sufficiently large such that it contains the target $\{Y_i^k\}_{i=1}^n$ for all k, when $\Delta \to 0$, minimizing the mean-related term in Eq. 3 implies

$$\mathbb{P}(Z_{\theta}^{k+1}(s, a) = \mathcal{T}^{opt}Q_{\theta^*}^k(s, a)) = 1, \tag{4}$$

where $\mathcal{T}^{opt}Q_{\theta^*}^k(s,a)$ is the scalar-valued target in the k-th phase of Neural FQI.

Proposition 3 demonstrates that as $\Delta \to 0$, the random variable $Z_{\theta}^{k+1}(s,a)$ with the limiting distribution in Neural FZI (distributional RL) will *degrade* to a constant

 $\mathcal{T}^{\text{opt}}Q_{\theta^*}^k(s,a)$, the minimizer (scalar-valued target) in Neural FQI (classical RL). That being said, minimizing the meanrelated term in Neural FZI is asymptotically equivalent to minimizing Neural FQI with the same limiting minimizer. A formal proof for convergence in distribution with the convergence rate $o(\Delta)$ is given in Appendix H. The realizable assumption that $\{Z_{\theta}: \theta \in \Theta\}$ is sufficiently large such that it contains $\{Y_i^k\}_{i=1}^n$ implies good in-distribution generalization performance in each phase of Neural FZI, which is also adopted in (Wu et al., 2023). This connection is also consistent with the mean-preserving property of distributional RL in the tabular setting (Rowland et al., 2018), but we extend this conclusion to the arbitrary function approximation with a histogram density estimator. Proposition 3 especially focuses on the asymptotic property of the mean-related term, which is different from existing convergence results based on the entire categorical distribution (Rowland et al., 2018; Bellemare et al., 2023). Given the connection between optimizing the mean-related term of Neural FZI with Neural FQI in Proposition 3, we can leverage the regularization term $\alpha \mathcal{H}(\widehat{\mu}^{s'_i,\pi_Z(s'_i)},q^{s_i,a_i}_{\theta})$ to explain the behavior difference between CDRL and classical RL, as analyzed later.

4.3. Uncertainty-aware Regularized Exploration

Regularization Effect. It turns out that minimizing the regularization term $\alpha \mathcal{H}(\widehat{\mu}^{s'_i,\pi_Z(s'_i)},q^{s_i,a_i}_{\theta})$ in Neural FZI pushes $q_{\scriptscriptstyle H}^{s,a}$ for the current return density estimator to catch up with the target return density function of $\hat{\mu}^{s'_i,\pi_Z(s'_i)}$. Importantly, $\widehat{\mu}^{s'_i,\pi_Z(s'_i)}$ encompasses the uncertainty of the entire return distribution in the learning course beyond only its expectation, given that $\hat{\mu}^{s'_i,\pi_Z(s'_i)}$ is the induced histogram density after applying the return density decomposition in Eq. 2. Since it is a prevalent notion that distributional RL can significantly reduce intrinsic uncertainty of the environment (Mavrin et al., 2019; Dabney et al., 2018a), the derived distribution-matching regularization term $\alpha \mathcal{H}(\widehat{\mu}^{s'_i,\pi_Z(s'_i)},q_{\theta}^{s_i,a_i})$ helps to capture more uncertainty of the environment by modeling higher moments of the whole return distribution beyond the expectation. In Section 5, we further demonstrate that this derived regularization contributes to an uncertainty-aware regularized exploration effect in the policy optimization or actor critic.

Remark: Approximation of $\widehat{\mu}^{s',\pi_Z(s')}$. In practical distributional RL algorithms, we typically use temporal-difference (TD) learning to attain the target probability density estimate $\widehat{\mu}^{s',\pi_Z(s')}$ based on Eq. 2, provided $\mathbb{E}\left[Z(s,a)\right]$ exists and $\epsilon \geq 1-p_E$ in Proposition 1. The approximation error of $\widehat{\mu}^{s',\pi_Z(s')}$ is fundamentally determined by the TD learning nature. A desirable approximation of $\widehat{\mu}^{s',\pi_Z(s')}$ intuitively leads to performance improvement in distributional RL. As KL divergence is used in CDRL, we also discuss the usage of KL divergence in distributional RL in Appendix F.

5. Regularization Benefits in Actor Critic

Notations. In this section, we use uppercase notation to represent random variables, such as $(\mathbf{s}_t, \mathbf{a}_t)$, at time t for clarity in the learning process of the actor critic.

5.1. Connection with MaxEnt RL

Motivation for the Connection. The maximum entropy regularization is commonly used in RL, which has various conceptual and practical advantages. Firstly, the learned policy is encouraged to visit states with high entropy in the future, promoting the exploration of diverse actions (Han & Sung, 2021; Haarnoja et al., 2018a; Williams & Peng, 1991). It also considerably improves the learning speed (Mei et al., 2020) and therefore is widely employed in state-of-the-art algorithms, e.g., Soft Actor-Critic (SAC) (Haarnoja et al., 2018a). Similar empirical benefits of both distributional RL and MaxEnt RL motivate us to probe their underlying connection, especially by comparing their exploration effects.

Explicit Entropy Regularization in MaxEnt RL. Max-Ent RL *explicitly* encourages exploration by optimizing for policies to reach states with higher entropy in the future:

$$J(\pi) = \sum_{t=0}^{T} \mathbb{E}_{(\mathbf{s}_{t}, \mathbf{a}_{t}) \sim \rho_{\pi}} \left[r\left(\mathbf{s}_{t}, \mathbf{a}_{t}\right) + \beta \mathcal{H}(\pi(\cdot|\mathbf{s}_{t})) \right], \quad (5)$$

where $\mathcal{H}\left(\pi_{\theta}\left(\cdot|\mathbf{s}_{t}\right)\right) = -\sum_{a} \pi_{\theta}\left(a|\mathbf{s}_{t}\right) \log \pi_{\theta}\left(a|\mathbf{s}_{t}\right)$ and ρ_{π} is the generated distribution following π . The temperature parameter β determines the relative importance of the entropy term against the cumulative rewards and thus controls the action diversity of the optimal policy learned via Eq. 5.

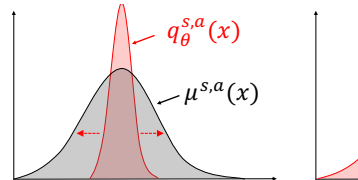
Implicit Entropy Regularization in Distributional RL. For a direct comparison with MaxEnt RL, it is required to specifically analyze the impact of the regularization term in Eq. 3. Therefore, we directly incorporate the distribution-matching regularization of distributional RL in Eq. 3 into the Actor Critic (AC) framework, enabling us to consider a new soft Q-value. The new Q function can be computed iteratively by applying a modified Bellman operator denoted as \mathcal{T}_d^π , called Distribution-Entropy-Regularized Bellman Operator. Given a fixed q_θ , \mathcal{T}_d^π is defined as

$$\mathcal{T}_{d}^{\pi}Q\left(\mathbf{s}_{t},\mathbf{a}_{t}\right) \triangleq r\left(\mathbf{s}_{t},\mathbf{a}_{t}\right) + \gamma \mathbb{E}_{\mathbf{s}_{t+1} \sim P\left(\cdot \mid \mathbf{s}_{t}, \mathbf{a}_{t}\right)}\left[V\left(\mathbf{s}_{t+1}\right)\right],\tag{6}$$

where a new soft value function $V(\mathbf{s}_t)$ is defined by

$$V\left(\mathbf{s}_{t}\right) = \mathbb{E}_{\mathbf{a}_{t} \sim \pi}\left[Q\left(\mathbf{s}_{t}, \mathbf{a}_{t}\right) + f\left(\mathcal{H}\left(\mu^{\mathbf{s}_{t}, \mathbf{a}_{t}}, q_{\theta}^{\mathbf{s}_{t}, \mathbf{a}_{t}}\right)\right)\right], \quad (7)$$

where f is a continuous increasing function over the crossentropy \mathcal{H} . $\mu^{\mathbf{s}_t,\mathbf{a}_t}$ is the induced true target return histogram density function via the decomposition in Eq. 2, which excludes its expectation. Note that $\mu^{\mathbf{s}_t,\mathbf{a}_t}$ can be approximated via bootstrap TD estimate $\widehat{\mu}^{\mathbf{s}_{t+1},\pi_Z(\mathbf{s}_{t+1})}$ similar to Eq. 3.



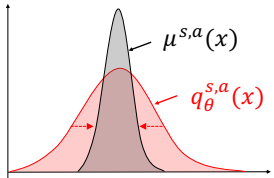


Figure 2: $q_{\theta}^{s,a}$ is optimized to disperse (left) or concentrate (right) to align with the uncertainty involved in target return distributions of $\mu^{s,a}$.

In this specific tabular setting regarding $\mathbf{s}_t, \mathbf{a}_t$, we particularly use $q_{\theta}^{\mathbf{s}_t, \mathbf{a}_t}$ to approximate the true density function of $Z(\mathbf{s}_t, \mathbf{a}_t)$. The f transformation over the cross-entropy \mathcal{H} between $\mu^{\mathbf{s}_t, \mathbf{a}_t}$ and $q_{\theta}^{\mathbf{s}_t, \mathbf{a}_t}(x)$ serves as the uncertainty-aware entropy regularization that we implicitly derive from value-based distributional RL in Section 4.2. By optimizing q_{θ} that is involved in the value-based critic component in actor critic, this regularization reduces the mismatch between the target return distribution and current estimate, aligning with the regularization effect analyzed in Section 4.3. As illustrated in Figure 2, $q_{\theta}^{s,a}$ is optimized to **catch up with** the uncertainty involved in the target return distribution of $\mu^{s,a}$, iteratively expanding the agent's knowledge about the environment uncertainty to contribute to more informative decisions. Next, we elaborate on its additional impact on policy learning in the actor critic in contrast to MaxEnt RL.

Reward Augmentation for Policy Learning. As opposed to the vanilla entropy regularization in MaxEnt RL that explicitly encourages the policy to explore, our derived regularization term in distributional loss of RL plays a role of reward augmentation for policy learning. Compared with classical RL, the augmented reward from the distributional loss incorporates additional knowledge of the return distribution in the learning process. As we will show later, the augmented reward encourages policies to reach states \mathbf{s}_t with actions $\mathbf{a}_t \sim \pi(\cdot|\mathbf{s}_t)$, whose current action-state return distribution $q_b^{\mathbf{s}_t,\mathbf{a}_t}$ lags far behind the (estimated) environmental uncertainty from the target returns.

For a detailed comparison with MaxEnt RL, we now focus on the properties of our decomposed distribution-matching regularization in the actor critic framework. In Lemma 1, we first demonstrate that our Distribution-Entropy-Regularized Bellman operator \mathcal{T}_d^π still inherits the convergence property in the policy evaluation phase with a cumulative augmented reward function as the new objective function $J'(\pi)$.

Lemma 1. (Distribution-Entropy-Regularized Policy Evaluation) Consider the distribution-entropy-regularized Bellman operator \mathcal{T}_d^{π} in Eq. 6 and assume $\mathcal{H}(\mu^{\mathbf{s}_t,\mathbf{a}_t},q_{\theta}^{\mathbf{s}_t,\mathbf{a}_t})$ is bounded for all $(\mathbf{s}_t,\mathbf{a}_t) \in \mathcal{S} \times \mathcal{A}$. We define $Q^{k+1} = \mathcal{T}_d^{\pi}Q^k$. Given q_{θ} , Q^{k+1} will converge to a corrected Q-value of π

as $k \to \infty$ with the new objective function $J'(\pi)$ defined as

$$J'(\pi) = \sum_{t=0}^{T} \mathbb{E}_{(\mathbf{s}_{t}, \mathbf{a}_{t}) \sim \rho_{\pi}} \left[r\left(\mathbf{s}_{t}, \mathbf{a}_{t}\right) + \gamma f(\mathcal{H}\left(\mu^{\mathbf{s}_{t}, \mathbf{a}_{t}}, q_{\theta}^{\mathbf{s}_{t}, \mathbf{a}_{t}}\right)) \right].$$
(8)

The updating rule in phase of policy optimization is $\pi_{\text{new}} = \arg\max_{\pi' \in \Pi} \mathbb{E}_{\mathbf{a}_t \sim \pi'} \left[Q^{\pi_{\text{old}}}(\mathbf{s}_t, \mathbf{a}_t) + f(\mathcal{H}(\mu^{\mathbf{s}_t, \mathbf{a}_t}, q_{\theta}^{\mathbf{s}_t, \mathbf{a}_t})) \right]$. Next, we derive a new policy iteration algorithm, called *Distribution-Entropy-Regularized Policy Iteration (DERPI)*, alternating between policy evaluation and policy improvement. It provably converges to a policy regularized by the distribution-matching term.

Theorem 1. (Distribution-Entropy-Regularized Policy Iteration) Repeatedly applying distribution-entropy-regularized policy evaluation in Eq. 6 and the policy improvement, the policy converges to an optimal policy π^* such that $Q^{\pi^*}(\mathbf{s}_t, \mathbf{a}_t) \geq Q^{\pi}(\mathbf{s}_t, \mathbf{a}_t)$ for all $\pi \in \Pi$.

Please refer to Appendix I for the proof of Lemma 1 and Theorem 1. Theorem 1 demonstrates that if we incorporate the decomposed regularization into the actor critic in Eq. 8, we can design a variant of "soft policy iteration" (Haarnoja et al., 2018a) that can guarantee the convergence to an optimal policy given any fixed q_{θ} . As a byproduct of our convergence analysis, we also extend DERPI to the function approximation setting provided in Appendix J, where we develop an interpretable algorithm. In summary, our theoretical investigation serves as the variant of the standard analytical framework in MaxEnt RL to allow a comparable analysis. Importantly, we next recognize a fundamental difference between our decomposed entropy regularization and the vanilla entropy regularization in MaxEnt RL.

Uncertainty-aware Regularized Exploration in CDRL Compared with MaxEnt RL. For the objective function $J(\pi)$ in Eq. 5 of MaxEnt RL, the state-wise entropy $\mathcal{H}(\pi(\cdot|\mathbf{s}_t))$ is maximized explicitly w.r.t. π for policies with a higher entropy in terms of diverse actions to encourage an explicit exploration. For the objective function $J'(\pi)$ in Eq. 8 of distributional RL, the policy π is implicitly optimized through the action selection process $\mathbf{a}_t \sim \pi(\cdot|\mathbf{s}_t)$ guided by an augmented reward signal from the distributionmatching regularization $f(\mathcal{H}(\mu^{\mathbf{s}_t, \mathbf{a}_t}, q_{\theta}^{\mathbf{s}_t, \mathbf{a}_t}))$. Concretely, the learned policy is encouraged to visit state s_t along with the policy-determined action via $\mathbf{a}_t \sim \pi(\cdot|\mathbf{s}_t)$, whose current action-state return distributions $q_{\theta}^{\mathbf{s}_t, \hat{\mathbf{a}}_t}$ lag far behind the target return distributions with a large discrepancy. This discrepancy is measured by the magnitude of the cross entropy between two return distributions of $q_{\theta}^{\mathbf{s}_t, \mathbf{a}_t}$ and $\mu^{\mathbf{s}_t, \mathbf{a}_t}$. A large discrepancy indicates that the uncertainty of current return distribution is considerably misestimated for considered states, enabling an uncertainty-aware exploration against these states in the policy optimization phase. This also indicates that the policy learning in CDRL is additionally driven by the uncertainty difference between the current and the target estimates, leading to a distinct exploration strategy of distributional RL relative to MaxEnt RL.

Interplay of Uncertainty-aware Regularization in Distributional Actor Critic. Putting the critic and actor learning together in distributional RL, we reveal their interplay impact pertinent to the uncertainty-aware regularized exploration when compared with classical RL. For the actor component, the policy learning seeks states and actions whose current return distribution estimate lags far behind the environmental uncertainty of the target returns. For the critic component, the critic learning reduces the return distribution mismatch on the states and actions explored by the policy, with two situations illustrated in Figure 2. This uncertainty-aware exploration effect arises from the decomposed regularization via the return density decomposition, interpreting the benefits of CDRL over classical RL.

6. Experiments

We provide a comprehensive demonstration of our theoretical analysis using both Atari games and MuJoCo tasks. In Section 6.1, we validate that the uncertainty-aware regularization is crucial to the outperformance of CDRL over classical RL by varying ϵ in the return density decomposition. Additionally, we investigate the mutual impacts between the vanilla entropy regularization in MaxEnt RL and the uncertainty-aware entropy regularization from CDRL in Section 6.2, with a slight extension to quantile-based distributional RL, e.g., Implicit Quantile Networks (IQN) (Dabney et al., 2018a). More implementation details, including the description of baselines, are provided in Appendix K.

6.1. Regularization Effect in Performance by Varying ϵ

Baseline Algorithm: $\mathcal{H}(\mu,q_{\theta})(\varepsilon=0.8/0.5/0.1)$. For the categorical distributional loss in C51 or the distributional critic loss in the actor critic, we employ $\widehat{\mu}^{s,a}$ instead of $\widehat{p}^{s,a}$ as the target return distribution, leading to the decomposed algorithms, denoted by $\mathcal{H}(\mu,q_{\theta})$. This decomposed algorithm enables us to assess the uncertainty-aware regularization effect of distributional RL by directly comparing its performance with the classical RL and CDRL.

Experimental Details. We substantiate that the decomposed uncertainty-aware entropy regularization, derived in Eq. 3 through the return density function decomposition, plays a crucial role in the empirical superiority of CDRL over classical RL. We compare CDRL with the decomposed baseline algorithm $\mathcal{H}(\mu, q_{\theta})$ under different ϵ based on Eq. 2. To ensure a pre-specified ϵ that guarantees a valid decomposition analyzed in Proposition 1, we employ a new notation ε , which shares the same utility as ϵ but is more convenient in the implementation. ε is defined as the mass proportion centered at the bin that contains the expectation when transporting the mass to other bins. A large proportion probability ε , which transports less mass to other bins, corresponds to a large ϵ in Eq. 2. Increasing ϵ indicates that the decomposed algorithm performs more similarly to a pure CDRL algorithm. See Appendix K.2 for more explanation, including the transformation equation between ϵ and ϵ , and the details of the baseline algorithm $\mathcal{H}(\mu, q_{\theta})$.

Results. Figure 3 showcases that as ε gradually decreases from 0.8 to 0.1, learning curves of decomposed C51, i.e., $\mathcal{H}(\mu, q_{\theta})(\varepsilon = 0.8/0.5/0.1)$, tend to degrade from C51 to DQN across most Atari games. The sensitivity of decomposed algorithm $\mathcal{H}(\mu, q_{\theta})$ regarding ε depends on the envi-

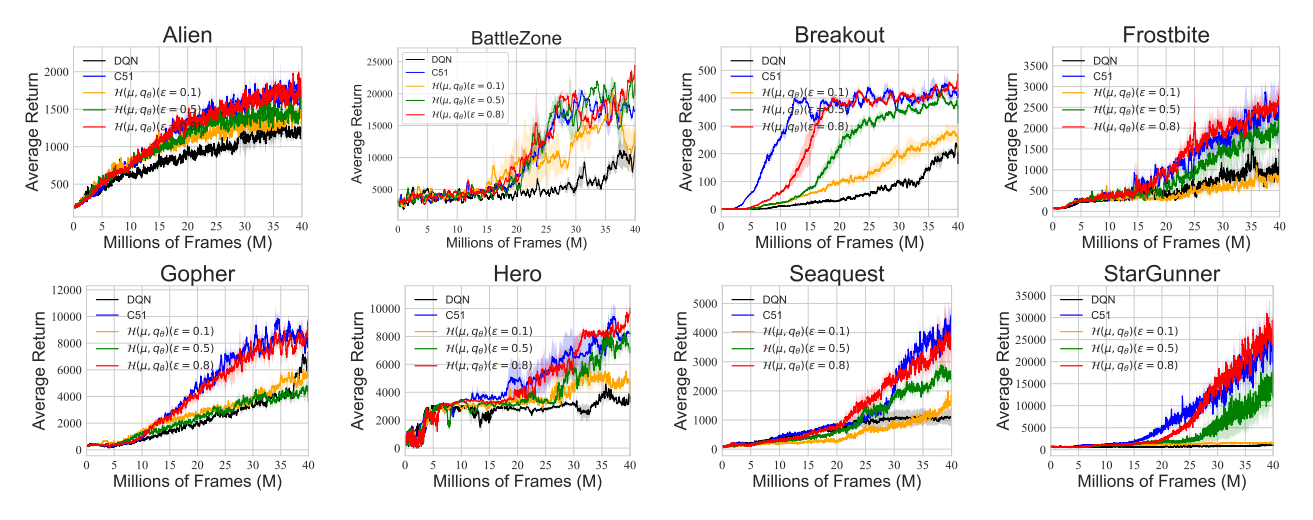


Figure 3: Learning curves of value-based CDRL, i.e., C51 algorithm, and the decomposed algorithm $\mathcal{H}(\mu, q_{\theta})(\varepsilon = 0.8/0.5/0.1)$ after applying the return distribution decomposition with different ε on eight Atari games. Results are averaged over three seeds, and the shade represents the standard deviation.

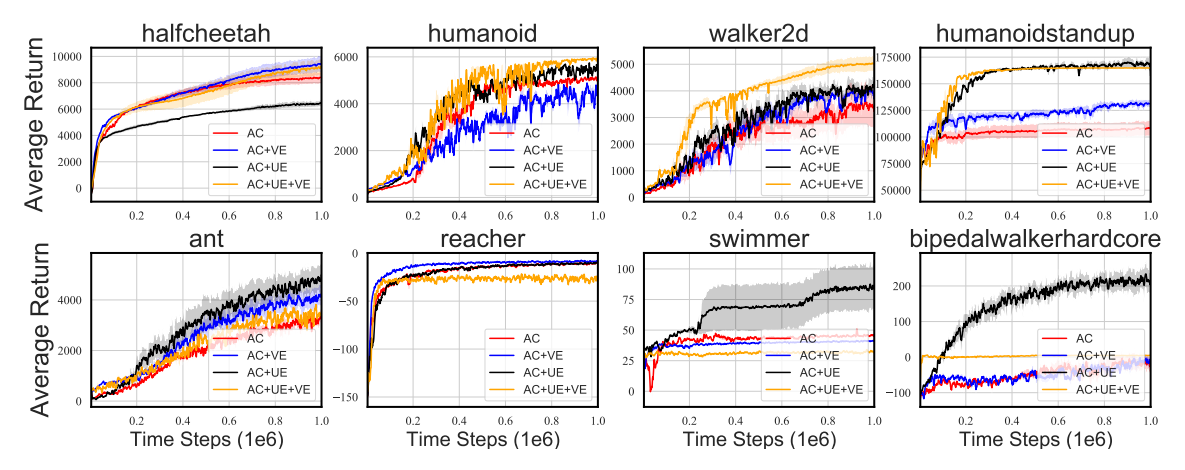


Figure 4: Learning curves of *AC*, *AC*+*VE* (SAC), *AC*+*UE* (DAC) and *AC*+*UE*+*VE* (DSAC) over five seeds across eight MuJoCo environments where DAC and DSAC are based on IQN. (**First Row**): Mutual improvement. (**Second Row**): Potential interference.

ronment. Similar results in MuJoCo environments can be found in Appendix L.1. Overall, our empirical result corroborates that the decomposed uncertainty-aware entropy regularization from the categorical distributional loss is pivotal to the empirical advantage of CDRL over classical RL.

6.2. Mutual Impacts of the Two Entropy Regularization

Baseline Algorithms. For a detailed comparison of the mutual impacts between Vanilla Entropy (VE) in MaxEnt RL and Uncertainty-aware Entropy (UE) in CDRL, we conduct an ablation study across several related baseline algorithms. We denote SAC with/without vanilla entropy as AC+VE and AC. We denote Distributional SAC (DSAC) (Ma et al., 2020) with/without vanilla entropy as AC+UE+VE and AC+UE. AC+UE is also denoted as DAC. The implementation details can be found in Appendix K.

Experimental Details. We demonstrate that the two types of regularized exploration in MaxEnt RL and CDRL play distinct roles in policy learning when employed simultaneously, including mutual improvement or potential interference. We perform our experiments for both DSAC (C51) and DSAC (IQN), where the latter is used to heuristically examine the mutual impacts in quantile-based distributional RL. Here, we present results on DSAC (IQN) and leave similar results on DSAC (C51) in Appendix L.2.

Results. In the first row of Figure 4, simultaneously employing uncertainty-aware and vanilla entropy regularization renders a mutual improvement. Conversely, the two kinds of regularizations, when adopted together, can also lead to performance degradation, as exhibited in the second row in Figure 4. For instance, on Swimmer and Reacher, AC+UE+VE is significantly inferior to AC+UE or AC+VE. We posit that the potential interference may result from dis-

tinct exploration directions in the policy learning for the two types of regularizations. SAC optimizes the policy to visit states with high entropy, while distributional RL updates the policy to explore states and the associated actions whose current return distribution estimate lags far behind the (estimated) environment uncertainty in target returns.

7. Extension to Quantile Distributional Loss

As an extension, we consider decomposing the quantile distributional loss, which is also commonly used in distributional RL, such as QR-DQN and IQN. Due to space limitations, a more detailed description is deferred to Appendix M. The quantile distributional loss can be viewed as a variant of composite quantile loss (Zou & Yuan, 2008). We commit to decomposing it into a mean-related term and a residual term, where the mean-related term is related to the expected quantile values. We demonstrate that minimizing the decomposed mean-related term is asymptotically mean-preserving (Rowland et al., 2019) as the number of quantiles approaches infinity. The induced residual term, therefore, captures the information from return distribution that excludes its expectation, serving as the benefit to explain the superiority of quantile-based distributional RL.

8. Conclusion and Discussion

In this study, we interpret the benefits of CDRL over classical RL as uncertainty-aware regularization via return density decomposition. In contrast to the exploration to encourage diverse actions in MaxEnt RL, the uncertainty-aware regularization in CDRL promotes exploring states where the environmental uncertainty is largely underestimated. Our study offers a novel exploration perspective to analyze the benefits of (categorical) distributional learning in RL.

Limitation and Future Work. The uncertainty-aware regularized exploration from distributional loss is mainly founded on CDRL. Although briefly examined in Section 7, it remains interesting yet challenging to extend our conclusion to general distributional RL, given that the analytical techniques, such as those in QR-DQN, are largely different from CDRL. We leave this extension for future work.

Impact Statement

This paper presents work whose goal is to advance the field of Machine Learning. There are many potential societal consequences of our work, none which we feel must be specifically highlighted here.

References

- Agrawal, R. and Horel, T. Optimal bounds between f-divergences and integral probability metrics. *Journal of Machine Learning Research*, 22(128):1–59, 2021.
- Arjovsky, M. and Bottou, L. Towards principled methods for training generative adversarial networks. *International Conference on Learning Representations*, 2017.
- Arjovsky, M., Chintala, S., and Bottou, L. Wasserstein generative adversarial networks. In *International conference on machine learning*, pp. 214–223. PMLR, 2017.
- Azizzadenesheli, K., Brunskill, E., and Anandkumar, A. Efficient exploration through bayesian deep q-networks. In 2018 Information Theory and Applications Workshop (ITA), pp. 1–9. IEEE, 2018.
- Bellemare, M. G., Dabney, W., and Munos, R. A distributional perspective on reinforcement learning. *International Conference on Machine Learning (ICML)*, 2017a.
- Bellemare, M. G., Danihelka, I., Dabney, W., Mohamed, S., Lakshminarayanan, B., Hoyer, S., and Munos, R. The cramer distance as a solution to biased wasserstein gradients. *arXiv preprint arXiv:1705.10743*, 2017b.
- Bellemare, M. G., Dabney, W., and Rowland, M. *Distributional reinforcement learning*. MIT Press, 2023.
- Chen, Y., Zhang, X., Wang, S., and Huang, L. Provable risk-sensitive distributional reinforcement learning with general function approximation. *International Conference on Machine Learning*, 2024.
- Cho, T., Han, S., Lee, H., Lee, K., and Lee, J. Pitfall of optimism: Distributional reinforcement learning by randomizing risk criterion. Advances in Neural Information Processing Systems, 2023.

- Dabney, W., Ostrovski, G., Silver, D., and Munos, R. Implicit quantile networks for distributional reinforcement learning. *International Conference on Machine Learning* (*ICML*), 2018a.
- Dabney, W., Rowland, M., Bellemare, M. G., and Munos,R. Distributional reinforcement learning with quantile regression. Association for the Advancement of Artificial Intelligence (AAAI), 2018b.
- Donsker, M. D. and Varadhan, S. S. Asymptotic evaluation of certain markov process expectations for large time—iii. *Communications on pure and applied Mathematics*, 29 (4):389–461, 1976.
- Fan, J., Wang, Z., Xie, Y., and Yang, Z. A theoretical analysis of deep q-learning. In *Learning for Dynamics and Control*, pp. 486–489. PMLR, 2020.
- Farebrother, J., Orbay, J., Vuong, Q., Taïga, A. A., Chebotar, Y., Xiao, T., Irpan, A., Levine, S., Castro, P. S., Faust, A., et al. Stop regressing: Training value functions via classification for scalable deep rl. arXiv preprint arXiv:2403.03950, 2024.
- Fujimoto, S., Hoof, H., and Meger, D. Addressing function approximation error in actor-critic methods. In *Interna*tional conference on machine learning, pp. 1587–1596. PMLR, 2018.
- Haarnoja, T., Tang, H., Abbeel, P., and Levine, S. Reinforcement learning with deep energy-based policies. In *International Conference on Machine Learning*, pp. 1352–1361. PMLR, 2017.
- Haarnoja, T., Zhou, A., Abbeel, P., and Levine, S. Soft actor-critic: Off-policy maximum entropy deep reinforcement learning with a stochastic actor. In *International* conference on machine learning, pp. 1861–1870. PMLR, 2018a.
- Haarnoja, T., Zhou, A., Hartikainen, K., Tucker, G., Ha, S., Tan, J., Kumar, V., Zhu, H., Gupta, A., Abbeel, P., et al. Soft actor-critic algorithms and applications. arXiv preprint arXiv:1812.05905, 2018b.
- Han, S. and Sung, Y. A max-min entropy framework for reinforcement learning. Advances in neural information processing systems (NeurIPS), 2021.
- Hao, J., Yang, T., Tang, H., Bai, C., Liu, J., Meng, Z., Liu, P., and Wang, Z. Exploration in deep reinforcement learning: From single-agent to multiagent domain. *IEEE Transactions on Neural Networks and Learning Systems*, 2023.
- Hinton, G., Vinyals, O., and Dean, J. Distilling the knowledge in a neural network. *NIPS Deep Learning Workshop*, 2015.

- Huber, P. J. Robust estimation of a location parameter. In *Breakthroughs in statistics: Methodology and distribution*, pp. 492–518. Springer, 1992.
- Huber, P. J. Robust Statistics, volume 523. John Wiley & Sons, 2004.
- Imani, E. and White, M. Improving regression performance with distributional losses. In *International Conference on Machine Learning*, pp. 2157–2166. PMLR, 2018.
- Jang, E., Gu, S., and Poole, B. Categorical reparameterization with gumbel-softmax. *International Conference on Learning Representations*, 2016.
- Kuang, Q., Zhu, Z., Zhang, L., and Zhou, F. Variance control for distributional reinforcement learning. *International Conference on Machine Learning*, 2023.
- Ladosz, P., Weng, L., Kim, M., and Oh, H. Exploration in deep reinforcement learning: A survey. *Information Fusion*, 85:1–22, 2022.
- Lee, K., Laskin, M., Srinivas, A., and Abbeel, P. Sunrise: A simple unified framework for ensemble learning in deep reinforcement learning. In *International Conference on Machine Learning*, pp. 6131–6141. PMLR, 2021.
- Lim, S. H. and Malik, I. Distributional reinforcement learning for risk-sensitive policies. Advances in Neural Information Processing Systems, 35:30977–30989, 2022.
- Lockwood, O. and Si, M. A review of uncertainty for deep reinforcement learning. In *Proceedings of the AAAI Conference on Artificial Intelligence and Interactive Digital Entertainment*, volume 18, pp. 155–162, 2022.
- Lyle, C., Bellemare, M. G., and Castro, P. S. A comparative analysis of expected and distributional reinforcement learning. In *Proceedings of the AAAI Conference on Artificial Intelligence*, volume 33, pp. 4504–4511, 2019.
- Ma, X., Xia, L., Zhou, Z., Yang, J., and Zhao, Q. Dsac: Distributional soft actor critic for risk-sensitive reinforcement learning. *arXiv* preprint arXiv:2004.14547, 2020.
- Ma, Y., Jayaraman, D., and Bastani, O. Conservative offline distributional reinforcement learning. Advances in neural information processing systems, 34:19235–19247, 2021.
- Mavrin, B., Zhang, S., Yao, H., Kong, L., Wu, K., and Yu, Y. Distributional reinforcement learning for efficient exploration. *International Conference on Machine Learning* (*ICML*), 2019.
- Mei, J., Xiao, C., Szepesvari, C., and Schuurmans, D. On the global convergence rates of softmax policy gradient methods. In *International Conference on Machine Learn*ing, pp. 6820–6829. PMLR, 2020.

- Metelli, A. M., Likmeta, A., and Restelli, M. Propagating uncertainty in reinforcement learning via wasserstein barycenters. *Advances in Neural Information Processing Systems*, 32, 2019.
- Mnih, V., Kavukcuoglu, K., Silver, D., Rusu, A. A., Veness, J., Bellemare, M. G., Graves, A., Riedmiller, M., Fidjeland, A. K., Ostrovski, G., et al. Human-level control through deep reinforcement learning. *nature*, 518(7540): 529–533, 2015.
- Mohri, M. Foundations of machine learning, 2018.
- Morimura, T., Sugiyama, M., Kashima, H., Hachiya, H., and Tanaka, T. Parametric return density estimation for reinforcement learning. *Proceedings of the Twenty-Sixth Conference on Uncertainty in Artificial Intelligence (UAI)*, 2011.
- Müller, R., Kornblith, S., and Hinton, G. When does label smoothing help? *Neural Information Processing Systems* (*NeurIPS*), 2019.
- Nguyen, T. T., Gupta, S., and Venkatesh, S. Distributional reinforcement learning with maximum mean discrepancy. *Association for the Advancement of Artificial Intelligence* (AAAI), 2020.
- Osband, I., Blundell, C., Pritzel, A., and Van Roy, B. Deep exploration via bootstrapped dqn. *Advances in neural information processing systems*, 29, 2016a.
- Osband, I., Van Roy, B., and Wen, Z. Generalization and exploration via randomized value functions. In *International Conference on Machine Learning*, pp. 2377–2386. PMLR, 2016b.
- Pan, Y., Banman, K., and White, M. Fuzzy tiling activations: A simple approach to learning sparse representations online. *International Conference on Learning Representations*, 2019.
- Riedmiller, M. Neural fitted q iteration–first experiences with a data efficient neural reinforcement learning method. In *European conference on machine learning*, pp. 317–328. Springer, 2005.
- Rowland, M., Bellemare, M., Dabney, W., Munos, R., and Teh, Y. W. An analysis of categorical distributional reinforcement learning. In *International Conference on Artificial Intelligence and Statistics*, pp. 29–37. PMLR, 2018.
- Rowland, M., Dadashi, R., Kumar, S., Munos, R., Bellemare, M. G., and Dabney, W. Statistics and samples in distributional reinforcement learning. *International Conference on Machine Learning (ICML)*, 2019.

- Rowland, M., Tang, Y., Lyle, C., Munos, R., Bellemare, M. G., and Dabney, W. The statistical benefits of quantile temporal-difference learning for value estimation. *International Conference on Machine Learning*, 2023.
- Rowland, M., Munos, R., Azar, M. G., Tang, Y., Ostrovski, G., Harutyunyan, A., Tuyls, K., Bellemare, M. G., and Dabney, W. An analysis of quantile temporal-difference learning. *Journal of Machine Learning Research (JMLR)*, 2024a.
- Rowland, M., Wenliang, L. K., Munos, R., Lyle, C., Tang, Y., and Dabney, W. Near-minimax-optimal distributional reinforcement learning with a generative model. *Advances in Neural Information Processing Systems* (NeurIPS), 2024b.
- Shi, C., Wang, X., Luo, S., Zhu, H., Ye, J., and Song, R. Dynamic causal effects evaluation in a/b testing with a reinforcement learning framework. *Journal of the American Statistical Association*, pp. 1–13, 2022.
- Sui, Y., Huang, Y., Zhu, H., and Zhou, F. Adversarial learning of distributional reinforcement learning. In *International Conference on Machine Learning*, pp. 32783–32796. PMLR. 2023.
- Sun, K., Liu, Y., Zhao, Y., Yao, H., Jui, S., and Kong, L. Exploring the training robustness of distributional reinforcement learning against noisy state observations. European Conference on Machine Learning and Principles and Practice of Knowledge Discovery in Databases (ECML-PKDD), 2023.
- Sun, K., Jiang, B., and Kong, L. How does return distribution in distributional reinforcement learning help optimization? In ICML 2024 Workshop: Aligning Reinforcement Learning Experimentalists and Theorists, 2024a.
- Sun, K., Zhao, Y., Liu, Y., Jiang, B., and Kong, L. Distributional reinforcement learning with regularized wasserstein distance. Advances in Neural Information Processing Systems, 2024b.
- Sutton, R. S. and Barto, A. G. *Reinforcement learning: An Introduction*. MIT press, 2018.
- Tang, Y. and Agrawal, S. Exploration by distributional reinforcement learning. *International Joint Conference on Artificial Intelligence (IJCAI)*, 2018.
- Wang, K., Zhou, K., Wu, R., Kallus, N., and Sun, W. The benefits of being distributional: Small-loss bounds for reinforcement learning. Advances in neural information processing systems, 2023.

- Wang, K., Oertell, O., Agarwal, A., Kallus, N., and Sun, W. More benefits of being distributional: Second-order bounds for reinforcement learning. *International Conference on Machine Learning*, 2024.
- Wasserman, L. *All of nonparametric statistics*. Springer Science & Business Media, 2006.
- Watkins, C. J. and Dayan, P. Q-learning. *Machine learning*, 8(3-4):279–292, 1992.
- Wenliang, L. K., Déletang, G., Aitchison, M., Hutter, M., Ruoss, A., Gretton, A., and Rowland, M. Distributional bellman operators over mean embeddings. *International Conference on Machine Learning*, 2024.
- Williams, R. J. and Peng, J. Function optimization using connectionist reinforcement learning algorithms. *Connection Science*, 3(3):241–268, 1991.
- Wiltzer, H., Bellemare, M. G., Meger, D., Shafto, P., and Jhaveri, Y. Action gaps and advantages in continuous-time distributional reinforcement learning. *Advances in Neural Information Processing Systems (NeurIPS)*, 2024a.
- Wiltzer, H., Farebrother, J., Gretton, A., and Rowland, M. Foundations of multivariate distributional reinforcement learning. *Advances in Neural Information Processing Systems (NeurIPS)*, 2024b.
- Wu, R., Uehara, M., and Sun, W. Distributional offline policy evaluation with predictive error guarantees. *International Conference on Machine Learning*, 2023.
- Yang, D., Zhao, L., Lin, Z., Qin, T., Bian, J., and Liu, T.-Y. Fully parameterized quantile function for distributional reinforcement learning. *Advances in neural information* processing systems, 32:6193–6202, 2019.
- Zhang, L., Peng, Y., Liang, J., Yang, W., and Zhang, Z. Estimation and inference in distributional reinforcement learning. *arXiv preprint arXiv:2309.17262*, 2023.
- Zhang, P., Chen, X., Zhao, L., Xiong, W., Qin, T., and Liu, T.-Y. Distributional reinforcement learning for multidimensional reward functions. *Advances in Neural Information Processing Systems*, 34:1519–1529, 2021.
- Zhou, F., Wang, J., and Feng, X. Non-crossing quantile regression for distributional reinforcement learning. *Advances in Neural Information Processing Systems*, 33, 2020.
- Zou, H. and Yuan, M. Composite quantile regression and the oracle model selection theory. *The Annals of Statistics*. *36* (*3*) *1108 1126*, 2008.

A. Related Work: More Discussions about Uncertainty-oriented Exploration in RL

Uncertainty in RL. Uncertainty is ubiquitous in RL and sequential decision-making, and therefore harnessing uncertainty is always crucial in designing efficient algorithms (Lockwood & Si, 2022). In the literature of uncertainty quantification, uncertainty is often decomposed into two sources: *aleatoric uncertainty* and *epistemic uncertainty*.

- Aleatoric uncertainty, also called intrinsic or environmental uncertainty, originates from the stochastic or probabilistic nature of the environment, encompassing three main sources: stochastic transition dynamics, stochastic policy, and stochastic reward function. Aleatoric uncertainty is determined by the environment, which is thus irreducible. However, we can design more efficient algorithms by capturing more environmental uncertainty in the learning process, e.g., via distributional RL.
- *Epistemic uncertainty*, also called parametric uncertainty, often originates from the stochasticity in statistical estimation in the presence of limited data or incomplete knowledge. As opposed to aleatoric uncertainty, epistemic uncertainty is reducible and should decrease over more data, which contributes to a more reliable statistical estimation.

Uncertainty-oriented Exploration. There are a few survey papers that comprehensively summarize existing exploration approaches (Ladosz et al., 2022; Hao et al., 2023). Following (Hao et al., 2023), we classify the exploration strategies into two main categories: *uncertainty-oriented exploration* and *intrinsic motivation-oriented exploration*. The latter is inspired by psychology, which is not the focus of our study. Importantly, according to the two categories of uncertainty in RL, uncertainty-oriented exploration, which often applies *Optimism in the Face of Uncertainty* (OFU) principle, involves aleatoric and epistemic uncertainty.

- Epistemic uncertainty-oriented exploration takes advantage of the uncertainty in the (posterior) estimation of value functions. The typical exploration methods include Bayesian framework (Osband et al., 2016b; Azizzadenesheli et al., 2018; Metelli et al., 2019), Bootstrap (Osband et al., 2016a), and Ensemble methods (Lee et al., 2021). For instance, Bootstrapped DQN (Osband et al., 2016a) maintains several independent Q-estimators and randomly samples one of them, enabling the agent to perform temporally extended exploration.
- Aleatoric uncertainty-oriented exploration aims to capture more environmental uncertainty from three sources of stochastic transition dynamics, stochastic policies, and stochastic reward function, all of which can be comprehensively integrated into return distribution. Cho et al. (2023) employs Perturbed Quantile Regression (PQR) to promote the optimistic exploration within the distributional RL framework, while Decaying Left Truncated Variance (DLTV) (Mavrin et al., 2019) utilizes the variance from the learned return distributions. Tang & Agrawal (2018) investigates the approximate posterior sampling in distributional RL to encourage the exploration. By contrast, our primal goal in this study is to attribute the benefits of distributional RL to its intrinsic uncertainty-aware exploration we derived via return density decomposition instead of harnessing the learned return distribution to develop subsequent aleatoric uncertainty-oriented exploration strategies in (Tang & Agrawal, 2018; Mavrin et al., 2019). On the other hand, MaxEnt RL (Haarnoja et al., 2017; 2018a;b) utilizes the stochasticity of learned policy, one of the three sources in environmental uncertainty, to encourage diverse actions. Therefore, MaxEnt RL can also be categorized into the aleatoric uncertainty-oriented exploration, and it is thus intuitive and interesting to make a detailed comparison of the exploration effects between distributional RL and MaxEnt RL, conducted in Section 5.1 of our study.

B. More Details about Categorical Distributional RL and Algorithm Description of C51

Distributional Loss and Projection in CDRL. Categorical Distributional RL (Bellemare et al., 2017a) uses the heuristic projection operator $\Pi_{\mathcal{C}}$, which was defined as

$$\Pi_{\mathcal{C}}(\delta_{y}) = \begin{cases}
\delta_{z_{1}} & y \leq z_{1} \\
\frac{z_{i+1} - y}{z_{i+1} - z_{i}} \delta_{l_{i}} + \frac{y - z_{i}}{z_{i+1} - z_{i}} \delta_{z_{i+1}} & z_{i} < y \leq z_{i+1} \\
\delta_{z_{N}} & y > z_{N}
\end{cases}$$
(9)

After applying the distributional Bellman operator \mathfrak{T}^{π} on the current return distribution $\eta^{\pi}(s,a)$ in each update, the resulting new distribution, which we denote as $\widetilde{\eta}^{\pi}(s,a)$, typically no longer lies in the same (discrete) support with the original one on $\{z_i\}_{i=1}^N$. To maintain the same support, the underpinning of the KL divergence, CDRL additionally applies the

projection operator $\Pi_{\mathcal{C}}$ on the new distribution $\widetilde{\eta}^{\pi}(s,a)$. This projection rule distributes the weight of δ_y across the original support points $\{z_i\}_{i=1}^N$ based on the linear interpolation. For example, if y lies in between two support points z_i and z_{i+1} , the probability mass on y is split between z_i and z_{i+1} with the weight inversely proportional to its distance ratio to z_i and z_{i+1} . Therefore, the projection extends affinely to finite mixtures of Dirac measures, such that for a mixture of Diracs $\sum_{i=1}^N p_i \delta_{y_i}$, we have $\Pi_{\mathcal{C}}\left(\sum_{i=1}^N p_i \delta_{y_i}\right) = \sum_{i=1}^N p_i \Pi_{\mathcal{C}}\left(\delta_{y_i}\right)$. The Cramér distance was recently studied as an alternative to the Wasserstein distances in the context of generative models (Bellemare et al., 2017b). Recall the definition of Cramér distance in the following.

Definition 1. (Definition 3 (Rowland et al., 2018)) The Cramér distance ℓ_2 between two distributions $\nu_1, \nu_2 \in \mathscr{P}(\mathbb{R})$, with cumulative distribution functions F_{ν_1}, F_{ν_2} respectively, is defined by:

$$\ell_2(\nu_1, \nu_2) = \left(\int_{\mathbb{R}} \left(F_{\nu_1}(x) - F_{\nu_2}(x) \right)^2 dx \right)^{1/2}.$$

Further, the supremum-Cramér metric $\bar{\ell}_2$ is defined between two distribution functions $\eta, \mu \in \mathscr{P}(\mathbb{R})^{\mathcal{X} \times \mathcal{A}}$ by

$$\bar{\ell}_2(\eta, \mu) = \sup_{(x,a) \in \mathcal{X} \times \mathcal{A}} \ell_2\left(\eta^{(x,a)}, \mu^{(x,a)}\right).$$

Thus, the contraction of categorical distributional RL can be guaranteed under Cramér distance:

Proposition 4. (Proposition 2 (Rowland et al., 2018)) The operator $\Pi_{\mathcal{C}}\mathcal{T}^{\pi}$ is a $\sqrt{\gamma}$ -contraction in $\bar{\ell}_2$.

An insight behind this conclusion is that Cramér distance endows a particular subset with a notion of orthogonal projection, and the orthogonal projection onto the subset is exactly the heuristic projection $\Pi_{\mathcal{C}}$ (Proposition 1 in (Rowland et al., 2018)). (Rowland et al., 2018) also states that the operator $\Pi_{\mathcal{C}}\mathcal{T}^{\pi}$ is contractive under Wasserstein distance.

Description of CDRL Algorithm: C51. With N=51, C51 instantiates the CDRL algorithm. To elaborate the algorithm, we first introduce the pushforward measure $f_{\#}\nu\in\mathcal{P}(\mathbb{R})$ from Definition 1 in (Rowland et al., 2018). This pushforward measure shifts the support of the probability measure μ according to the map f, which is commonly used in distributional RL literature. In particular, we consider an affine shift map $f_{r,\gamma}:\mathbb{R}\to\mathbb{R}$, defined by $f_{r,\gamma}(x)=r+\gamma x$. As Algorithm 1 displays, we first apply the pushforward measure on the target return distribution $\widehat{\eta}(s',a^*)$ by affinely shifting its support points, leading to a new distribution $\widehat{\eta}(s,a)$. Next, we project the support points of $\widehat{\eta}(s,a)$ by employing $\Pi_{\mathcal{C}}$ onto the original support, allowing us to compute the KL divergence in the end. Notably, we decompose the distributional objective function on the KL loss $\mathrm{KL}(\widehat{\eta}_{\mathrm{target}}(s,a)||\widehat{\eta}(s,a))$.

Algorithm 1 CDRL Update (Adapted from Algorithm 1 in (Rowland et al., 2018))

Require: Number of atoms N, e.g., N=51 in C51, the categorical distribution $\widehat{\eta}(s,a)=\sum_{i=1}^N p_i^{s,a}\delta_{z_i}$ for the current return distribution.

Input: Sample transition (s, a, r, s')

1: if Policy evaluation: then

2: $a^* \sim \pi(\cdot|s')$

3: **else if** Control: **then**

4: $a^* \leftarrow \arg\max_{a' \in \mathcal{A}} \mathbb{E}_{R \sim \widehat{n}(s', a')}[R]$

5: end if

6: $\widetilde{\eta}(s,a) \leftarrow (f_{r,\gamma})_{\#} \widehat{\eta}(s',a^*) \# \text{ Distributional Bellmen update by applying } \widehat{\mathfrak{T}}^{\pi}$

7: $\widehat{\eta}_{\text{target}}(s, a) \leftarrow \Pi_{\mathcal{C}} \widetilde{\eta}(s, a) \# \text{Project target support points and then distribute the probabilities}$

Output: Compute the distributional loss $\mathrm{KL}(\widehat{\eta}_{\mathrm{target}}(s,a)||\widehat{\eta}(s,a))$ # Choose KL divergence as d_p

C. Proof of Proposition 1

Proposition 1.(Decomposition Validity) Denote $\widehat{p}^{s,a}(x \in \Delta_E) = p_E/\Delta$, where p_E is the coefficient on the bin Δ_E . $\widehat{\mu}^{s,a}(x) = \sum_{i=1}^N p_i^\mu \mathbb{1}(x \in \Delta_i)/\Delta$ is a valid density if and only if $\epsilon \geq 1 - p_E$.

Proof. Recap a valid probability density function requires non-negative and one-bounded probability in each bin and all probabilities should sum to 1.

Necessity. (1) When $x \in \Delta_E$, Eq. 2 can simplified as $p_E/\Delta = (1-\epsilon)/\Delta + \epsilon p_E^\mu/\Delta$, where $p_E^\mu = \widehat{\mu}(x \in \Delta_E)$. Thus, $p_E^\mu = \frac{p_E}{\epsilon} - \frac{1-\epsilon}{\epsilon} \geq 0$ if $\epsilon \geq 1-p_E$. Obviously, $p_E^\mu = \frac{p_E}{\epsilon} - \frac{1-\epsilon}{\epsilon} \leq \frac{1}{\epsilon} - \frac{1-\epsilon}{\epsilon} = 1$ guaranteed by the validity of $\widehat{p}_E^{s,a}$. (2) When $x \notin \Delta_E$, we have $p_i/\Delta = \epsilon p_i^\mu/\Delta$, i.e., When $x \notin \Delta_E$, We immediately have $p_i^\mu = \frac{p_i}{\epsilon} \leq \frac{1-p_E}{\epsilon} \leq 1$ when $\epsilon \geq 1-p_E$. Also, $p_i^\mu = \frac{p_i}{\epsilon} \geq 0$.

Sufficiency. (1) When $x \in \Delta_E$, let $p_E^\mu = \frac{p_E}{\epsilon} - \frac{1-\epsilon}{\epsilon} \ge 0$, we have $\epsilon \ge 1 - p_E$. $p_E^\mu = \frac{p_E}{\epsilon} - \frac{1-\epsilon}{\epsilon} \le 1$ in nature. (2) When $x \notin \Delta_E$, $p_i^\mu = \frac{p_i}{\epsilon} \ge 0$ in nature. Let $p_i^\mu = \frac{p_i}{\epsilon} \le 1$, we have $p_i \le \epsilon$. We need to take the intersection set of (1) and (2), and we find that $\epsilon \ge 1 - p_E \Rightarrow \epsilon \ge 1 - p_E \ge p_i$ that satisfies the condition in (2). Thus, the intersection set of (1) and (2) would be $\epsilon \ge 1 - p_E$.

In summary, as $\epsilon \geq 1 - p_E$ is both the necessary and sufficient condition, we have the conclusion that $\widehat{\mu}(x)$ is a valid probability density function $\iff \epsilon \geq 1 - p_E$.

D. Equivalence between Categorical Parameterization and Histogram Density Estimation in Distributional RL

Proposition 5. Suppose the target categorical distribution $c = \sum_{i=1}^{N} p_i \delta_{z_i}$ and the target histogram function $h(x) = \sum_{i=1}^{N} p_i \mathbb{1}(x \in \Delta_i)/\Delta$, updating the parameterized categorical distribution c_{θ} under KL divergence is equivalent to updating the parameterized histogram function h_{θ} .

Proof. For the histogram density estimator h_{θ} and the true target density function p(x), we can simplify the KL divergence as follows.

$$D_{KL}(h, h_{\theta}) = \sum_{i=1}^{N} \int_{l_{i-1}}^{l_{i}} \frac{p_{i}(x)}{\Delta} \log \frac{\frac{p_{i}(x)}{\Delta}}{\frac{h_{\theta}^{i}}{\Delta}} dx$$

$$= \sum_{i=1}^{N} \int_{l_{i-1}}^{l_{i}} \frac{p_{i}(x)}{\Delta} \log \frac{p_{i}(x)}{\Delta} dx - \sum_{i=1}^{N} \int_{l_{i-1}}^{l_{i}} \frac{p_{i}(x)}{\Delta} \log \frac{h_{\theta}^{i}}{\Delta} dx$$

$$\stackrel{(a)}{\propto} - \sum_{i=1}^{N} \int_{l_{i-1}}^{l_{i}} \frac{p_{i}(x)}{\Delta} \log \frac{h_{\theta}^{i}}{\Delta} dx$$

$$\stackrel{(b)}{=} - \sum_{i=1}^{N} p_{i} \log \frac{h_{\theta}^{i}}{\Delta}$$

$$\stackrel{(c)}{\propto} - \sum_{i=1}^{N} p_{i} \log h_{\theta}^{i}$$

$$(10)$$

where h_{θ}^{i} is determined by i and θ , which is independent of x. (a) is true because the target distribution with all p_{i} is fixed. (b) follows because $p_{i}(x)$ remains constant for $x \in [l_{i}, l_{i+1}]$. Finally, (c) holds as the remaining term involving p_{i} , and Δ is also constant.

On the other hand, we consider the KL-based objective function in learning categorical distribution estimator. Given the target categorical distribution $c = \sum_{i=1}^{N} p_i \delta_{z_i}$, where the probability p_i is fixed for each atom z_i , we aim at updating the current categorical estimator c_{θ} . Then, we have:

$$D_{KL}(c, c_{\theta}) = \sum_{i=1}^{N} p_i \log \frac{p_i}{c_{\theta}^i} = \sum_{i=1}^{N} p_i \log p_i - \sum_{i=1}^{N} p_i \log c_{\theta}^i \propto -\sum_{i=1}^{N} p_i \log c_{\theta}^i,$$
(11)

where $c_{\theta} = \sum_{i=1}^{N} c_{\theta}^{i} \delta_{z_{i}}$ is the current categorical estimator and c_{θ}^{i} is the learnable probability. By comparing the final loss function forms in Eq. 10 and Eq. 11, it turns out that they are equivalent as both c_{θ}^{i} and h_{θ}^{i} are the learnable probabilities, which are parameterized by the same neural network.

Remark. In CDRL, we use a discrete categorical distribution with probabilities centered on the fixed atoms $\{z_i\}_{i=1}^N$. In contrast, the histogram density estimator in our analysis is a continuous function defined on $[z_0, z_N]$, enabling more nuanced analysis within continuous functions. Proposition 5 indicates that minimizing the KL divergence with the categorical distribution in Eq. 11 amounts to the cross-entropy loss with the parameterized histogram function in Eq. 10.

E. Convergence Guarantee of Histogram Density Estimator in Distributional RL

Histogram Function Parameterization Error: Uniform Convergence in Probability. The previous discrete categorical parameterization error bound in (Rowland et al., 2018) (Proposition 3) is derived between the true return distribution and the limiting return distribution denoted as η_C iteratively updated via the Bellman operator $\Pi_C \mathfrak{T}^\pi$ in expectation, without considering an asymptotic analysis when the number of sampled $\{s_i, a_i\}_{i=1}^n$ pairs goes to infinity. As a complementary result, we provide a uniform convergence rate for the histogram density estimator in the context of distributional RL. In this particular analysis within this subsection, we denote $\widehat{p}_C^{s,a}$ as the density function estimator for the true limiting return distribution η_C via $\Pi_C \mathfrak{T}^\pi$ with its true density $p_C^{s,a}$. In Theorem 2, we show that the sample-based histogram estimator $\widehat{p}_C^{s,a}$ can approximate any arbitrary continuous limiting density function $p_C^{s,a}$ under a mild condition. This ensures the use of a histogram density estimator in the implementation of our subsequent algorithm adapted from CDRL.

Theorem 2. (Uniform Convergence Rate in Probability) Suppose $p_{\mathcal{C}}^{s,a}(x)$ is Lipschitz continuous, and the support of a random variable is partitioned by N bins with bin size Δ . Then

$$\sup_{x} |\widehat{p}_{\mathcal{C}}^{s,a}(x) - p_{\mathcal{C}}^{s,a}(x)| = O(\Delta) + O_P\left(\sqrt{\frac{\log N}{n\Delta^2}}\right).$$
 (12)

Proof. Our proof is mainly based on the non-parametric statistics analysis (Wasserman, 2006). In particular, the difference of $\hat{p}_{\mathcal{C}}^{s,a}(x) - p_{\mathcal{C}}^{s,a}(x)$ can be written as

$$\widehat{p}_{\mathcal{C}}^{s,a}(x) - p_{\mathcal{C}}^{s,a}(x) = \underbrace{\mathbb{E}\left(\widehat{p}_{\mathcal{C}}^{s,a}(x)\right) - p_{\mathcal{C}}^{s,a}(x)}_{\text{bias}} + \underbrace{\widehat{p}_{\mathcal{C}}^{s,a}(x) - \mathbb{E}\left(\widehat{p}_{\mathcal{C}}^{s,a}(x)\right)}_{\text{stochastic variation}}.$$
(13)

(1) The first bias term. Without loss of generality, we consider $x \in \Delta_k$, we have

$$\mathbb{E}\left(\widehat{p}_{\mathcal{C}}^{s,a}(x)\right) = \frac{P(X \in \Delta_{k})}{\Delta}$$

$$= \frac{\int_{l_{0}+(k-1)\Delta}^{l_{0}+k\Delta} p(y)dy}{\Delta}$$

$$= \frac{F(l_{0}+(k-1)\Delta) - F(l_{0}+(k-1)\Delta)}{l_{0}+k\Delta - (l_{0}+(k-1)\Delta)}$$

$$= p_{\mathcal{C}}^{s,a}(x'),$$
(14)

where the last equality is based on the mean value theorem. According to the L-Lipschitz continuity property, we have

$$|\mathbb{E}\left(\hat{p}_{\mathcal{C}}^{s,a}(x)\right) - p_{\mathcal{C}}^{s,a}(x)| = |p_{\mathcal{C}}^{s,a}(x') - p_{\mathcal{C}}^{s,a}(x)| \le L|x' - x| \le L\Delta$$
(15)

(2) The second stochastic variation term. If we let $x \in \Delta_k$, then $\widehat{p}_{\mathcal{C}}^{s,a} = p_k = \frac{1}{n} \sum_{i=1}^n \mathbb{1}(X_i \in \Delta_k)$, we thus have

$$P\left(\sup_{x} |\widehat{p}_{\mathcal{C}}^{s,a}(x) - \mathbb{E}\left(\widehat{p}_{\mathcal{C}}^{s,a}(x)\right)| > \epsilon\right)$$

$$= P\left(\max_{j=1,\dots,N} \left| \frac{1}{n} \sum_{i=1}^{n} \mathbb{1}\left(X_{i} \in \Delta_{j}\right) / \Delta - P\left(X_{i} \in \Delta_{j}\right) / \Delta\right| > \epsilon\right)$$

$$= P\left(\max_{j=1,\dots,N} \left| \frac{1}{n} \sum_{i=1}^{n} \mathbb{1}\left(X_{i} \in \Delta_{j}\right) - P\left(X_{i} \in \Delta_{j}\right)\right| > \Delta\epsilon\right)$$

$$\leq \sum_{j=1}^{N} P\left(\left| \frac{1}{n} \sum_{i=1}^{n} \mathbb{1}\left(X_{i} \in \Delta_{j}\right) - P\left(X_{i} \in \Delta_{j}\right)\right| > \Delta\epsilon\right)$$

$$\leq N \cdot \exp\left(-2n\Delta^{2}\epsilon^{2}\right) \quad \text{(by Hoeffding's inequality)},$$

$$(16)$$

where in the last inequality we know that the indicator function is bounded in [0, 1]. We then let the last term be a constant independent of N, n, Δ and simplify the order of ϵ . Then, we have:

$$\sup_{x} |\widehat{p}_{\mathcal{C}}^{s,a}(x) - \mathbb{E}\left(\widehat{p}_{\mathcal{C}}^{s,a}(x)\right)| = O_{P}\left(\sqrt{\frac{\log N}{n\Delta^{2}}}\right)$$
(17)

In summary, as the above inequality holds for each x, we thus have the uniform convergence rate of a histogram density estimator

$$\sup_{x} |\widehat{p}_{\mathcal{C}}^{s,a}(x) - p_{\mathcal{C}}^{s,a}(x)| \leq \sup_{x} |\mathbb{E}\left(\widehat{p}_{\mathcal{C}}^{s,a}(x)\right) - p_{\mathcal{C}}^{s,a}(x)| + \sup_{x} |\widehat{p}_{\mathcal{C}}^{s,a}(x) - \mathbb{E}\left(\widehat{p}_{\mathcal{C}}^{s,a}(x)\right)|$$

$$= O\left(\Delta\right) + O_{P}\left(\sqrt{\frac{\log N}{n\Delta^{2}}}\right). \tag{18}$$

F. Discussion about KL Divergence in Distributional RL

F.1. Properties of KL divergence in Distributional RL

Remark on KL Divergence. As stated in Section 3 of CDRL (Bellemare et al., 2017a), when the categorical parameterization is applied after the projection operator $\Pi_{\mathcal{C}}$, the distributional Bellman operator \mathfrak{T}^{π} has the contraction guarantee under Cramér distance or Wasserstein distance (Rowland et al., 2018), albeit the direct use of a non-expansive KL divergence (Morimura et al., 2011). Similarly, our histogram density parameterization with the projection $\Pi_{\mathcal{C}}$ and KL divergence also enjoys a contraction property due to the equivalence between optimizing histogram function and categorical distribution analyzed in Appendix D. We summarize some properties of KL divergence in distributional RL in Proposition 6.

Proposition 6. Given two probability measures μ and ν , we define the supreme D_{KL} as a functional $\mathcal{P}(\mathcal{X})^{S \times A} \times \mathcal{P}(\mathcal{X})^{S \times A} \to \mathbb{R}$, i.e., $D_{KL}^{\infty}(\mu, \nu) = \sup_{(s,a) \in \mathcal{S} \times A} D_{KL}(\mu(s,a), \nu(s,a))$. we have:

(1) \mathfrak{T}^{π} is a non-expansive distributional Bellman operator under D_{KL}^{∞} , i.e.,

$$D_{KL}^{\infty}(\mathfrak{T}^{\pi}Z_1,\mathfrak{T}^{\pi}Z_2) \le D_{KL}^{\infty}(Z_1,Z_2),\tag{19}$$

(2) $D_{\mathit{KL}}^{\infty}(Z_n,Z) \to 0$ implies the Wasserstein distance $W_p(Z_n,Z) \to 0$.

Proof. We first assume Z_{θ} is absolutely continuous and the supports of two distributions in KL divergence have a negligible intersection (Arjovsky & Bottou, 2017), under which the KL divergence is well-defined.

(1) The contraction analysis of distributional Bellman operator \mathfrak{T}^{π} under a distribution divergence d_p depends on its *scale sensitive* (S) and *sum invariant* (I) properties (Bellemare et al., 2017b;a). We say d_p is scale sensitive (of order τ) if there exists a $\tau > 0$, such that for all random variables X, Y and a real value a > 0, $d_p(aX, aY) \le |a|^{\tau} d_p(X, Y)$. d_p has the sum invariant property if whenever a random variable A is independent from X, Y, we have $d_p(A + X, A + Y) \le d_p(X, Y)$. We first prove that the D_{KL} is sum-invariant, which is based on the dual form of KL divergence via the variational representation (Donsker & Varadhan, 1976; Agrawal & Horel, 2021):

$$D_{\mathrm{KL}}(X,Y) = \sup_{f \in \mathcal{L}^b} \{ \mathbb{E}_X[f(x)] - \log\left(\mathbb{E}_Y\left[e^{f(y)}\right]\right) \},\tag{20}$$

where \mathcal{L}^b is the space of bounded measurable functions. Consequently, we have

$$D_{KL}(A + X, A + Y) = \sup_{f \in \mathcal{L}^{b}} \{\mathbb{E}_{Z_{1} = A + X}[f(z_{1})] - \log\left(\mathbb{E}_{Z_{2} = A + Y}\left[e^{f(z_{2})}\right]\right)\}$$

$$\stackrel{(a)}{=} \sup_{f \in \mathcal{L}^{b}} \{\mathbb{E}_{A}\left[\mathbb{E}_{X}\left[f(x + a)\right]\right] - \log\left(\mathbb{E}_{A}\left[\mathbb{E}_{Y}\left[e^{f(y + a)}\right]\right]\right)\}$$

$$\stackrel{(b)}{\leq} \sup_{f \in \mathcal{L}^{b}} \{\mathbb{E}_{A}\mathbb{E}_{X}[f(x + a)] - \mathbb{E}_{A}\log\left(\mathbb{E}_{Y}\left[e^{f(y + a)}\right]\right)\}$$

$$= \sup_{f \in \mathcal{L}^{b}} \{\mathbb{E}_{A}[\mathbb{E}_{X}[f(x + a)] - \log\left(\mathbb{E}_{Y}\left[e^{f(y + a)}\right]\right)]\}$$

$$\stackrel{(c)}{\leq} \mathbb{E}_{A} \sup_{f \in \mathcal{L}^{b}} \{\mathbb{E}_{X}[f(x + a)] - \log\left(\mathbb{E}_{Y}\left[e^{f(y + a)}\right]\right)\}$$

$$\stackrel{(d)}{=} \mathbb{E}_{A} \sup_{g \in \mathcal{L}^{b}} \{\mathbb{E}_{X}[g(x)] - \log\left(\mathbb{E}_{Y}\left[e^{g(y)}\right]\right)\}$$

$$= D_{KL}(X, Y),$$

where (a) results from the independence between A and X (Y). (b) and (c) rely on the Jensen inequality for the function $-\log$ and the operator \sup . (d) is because the translation is still within the same bounded functional space. Next, we show that D_{KL} is not scale-sensitive, where we denote the probability density function of X and Y as P and P.

$$D_{KL}(aX, aY) = \int_{-\infty}^{\infty} \frac{1}{a} p\left(\frac{x}{a}\right) \log \frac{\frac{1}{a} p\left(\frac{x}{a}\right)}{\frac{1}{a} q\left(\frac{x}{a}\right)} dx = \int_{-\infty}^{\infty} p(y) \log \frac{p(y)}{q(y)} dy = D_{KL}(X, Y)$$
 (22)

Putting the two properties together and given two return distributions $Z_1(s, a)$ and $Z_2(s, a)$, we have the non-expansive contraction property of the supremal form of D_{KL} as follows.

$$D_{KL}^{\infty}(\mathfrak{T}^{\pi}Z_{1},\mathfrak{T}^{\pi}Z_{2}) = \sup_{s,a} D_{KL}(\mathfrak{T}^{\pi}Z_{1}(s,a),\mathfrak{T}^{\pi}Z_{2}(s,a))$$

$$= \sup_{s,a} D_{KL}(R(s,a) + \gamma Z_{1}(s',a'), R(s,a) + \gamma Z_{2}(s',a'))$$

$$\stackrel{(a)}{\leq} D_{KL}(\gamma Z_{1}(s',a'), \gamma Z_{2}(s',a'))$$

$$\stackrel{(b)}{=} D_{KL}(Z_{1}(s',a'), Z_{2}(s',a'))$$

$$\leq \sup_{s,a} D_{KL}(Z_{1}(s',a'), Z_{2}(s',a'))$$

$$= D_{VI}^{\omega}(Z_{1}, Z_{2}).$$
(23)

where (a) relies on the sum invariant property of D_{KL} and (b) utilizes the non-scale sensitive property of D_{KL} . By applying the well-known Banach fixed point theorem, we have a unique return distribution when convergence of distributional dynamic programming under D_{KL}^{∞} .

(2) By the definition of D_{KL}^{∞} , we have $\sup_{s,a} D_{\mathrm{KL}}(Z_n(s,a),Z(s,a)) \to 0$ implies $D_{\mathrm{KL}}(Z_n,Z) \to 0$. $D_{\mathrm{KL}}(Z_n,Z) \to 0$ implies the total variation distance $\delta(Z_n,Z) \to 0$ according to a straightforward application of Pinsker's inequality

$$\delta\left(Z_{n},Z\right) \leq \sqrt{\frac{1}{2}D_{\mathrm{KL}}\left(Z_{n},Z\right)} \to 0, \quad \delta\left(Z,Z_{n}\right) \leq \sqrt{\frac{1}{2}D_{\mathrm{KL}}\left(Z,Z_{n}\right)} \to 0 \tag{24}$$

Based on Theorem 2 in WGAN (Arjovsky et al., 2017), $\delta(Z_n, Z) \to 0$ implies $W_p(Z_n, Z) \to 0$. This is trivial by recalling the fact that δ and W give the strong and weak topologies on the dual of $(C(\mathcal{X}), \|\cdot\|_{\infty})$ when restricted to $Prob(\mathcal{X})$.

F.2. Equivalence between Cross-Entropy Loss and KL Divergence in Neural FZI

If the target density function in evaluating the KL divergence is not fixed, using cross-entropy loss instead of the KL divergence may underestimate the uncertainty of return since this simplification may fail to capture the exact shape or

uncertainty spread of the true target return distribution. However, this underestimation issue does occur in our analysis. Particularly, the leverage of the target network in Neural FZI, which is fixed in the updating of each phase, guarantees that the KL divergence is *exactly* proportional to the cross-entropy loss. Figure 5 suggests that C51 with cross-entropy loss (DSAC_CE) behaves similarly to the vanilla C51 equipped with KL divergence (DSAC) in both three Atari games and MuJoCo environments with continuous action space.

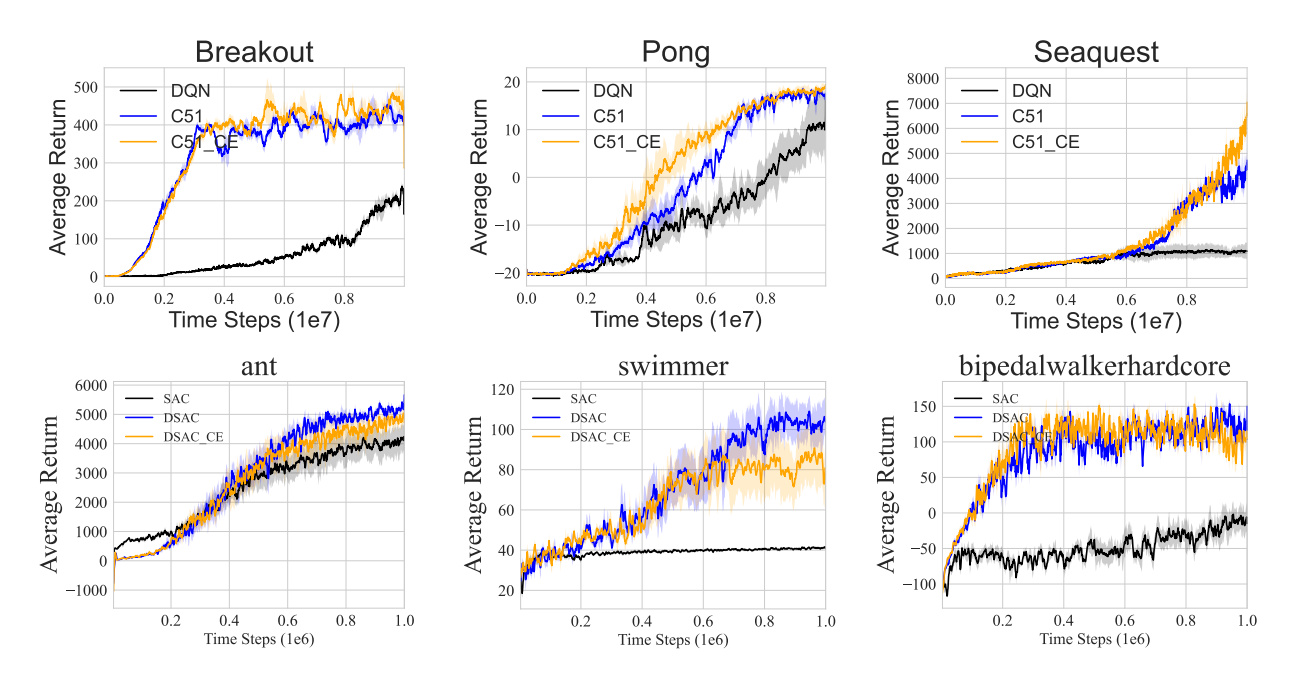


Figure 5: (**First row**) Learning curves of C51 under cross-entropy loss on Atari games over 3 seeds. (**Second row**) Learning curves of DSAC with C51 under cross-entropy loss on MuJoCo environments over five seeds.

G. Proof of Proposition 2

Proposition 2 (Decomposed Neural FZI) Denote $q_{\theta}^{s,a}$ as the histogram density function of $Z_{\theta}^{k}(s,a)$ in Neural FZI. Based on Eq. 2 and KL divergence as d_{p} , Neural FZI in Eq. 1 is simplified as

$$Z_{\theta}^{k+1} = \underset{q_{\theta}}{\operatorname{argmin}} \frac{1}{n} \sum_{i=1}^{n} \left[\underbrace{-\log q_{\theta}^{s_i, a_i}(\Delta_E^i)}_{(a)} + \alpha \mathcal{H}(\widehat{\mu}^{s_i', \pi_Z(s_i')}, q_{\theta}^{s_i, a_i}) \right]. \tag{25}$$

Proof. Firstly, given a fixed p(x) we know that minimizing $D_{KL}(p,q_{\theta})$ is equivalent to minimizing $\mathcal{H}(p,q)$ by following

$$D_{KL}(p, q_{\theta}) = \sum_{i=1}^{N} \int_{l_{i-1}}^{l_{i}} \frac{p_{i}(x)}{\Delta} \log \frac{p^{i}(x)/\Delta}{q_{\theta}^{i}/\Delta} dx$$

$$= -\sum_{i=1}^{N} \int_{l_{i-1}}^{l_{i}} \frac{p_{i}(x)}{\Delta} \log \frac{q_{\theta}^{i}}{\Delta} dx - (\sum_{i=1}^{N} \int_{l_{i-1}}^{l_{i}} \frac{p_{i}(x)}{\Delta} \log \frac{p^{i}(x)}{\Delta} dx)$$

$$= \mathcal{H}(p, q_{\theta}) - \mathcal{H}(p)$$

$$\propto \mathcal{H}(p, q_{\theta})$$
(26)

where $p = \sum_{i=1}^N p_i(x) \mathbb{1}(x \in \Delta^i)/\Delta$ and $q_\theta = \sum_{i=1}^N q_i/\Delta$. Based on $\mathcal{H}(p,q_\theta)$, we use $p^{s_i',\pi_Z(s_i')}(x)$ to denote the target probability density function of the random variable $\mathcal{R}(s_i,a_i) + \gamma Z_{\theta^*}^k(s_i',\pi_Z(s_i'))$. Then, we can derive the objective

function within each Neural FZI as

$$\frac{1}{n} \sum_{i=1}^{n} \mathcal{H}(p^{s'_{i},\pi_{Z}(s'_{i})}, q^{s_{i},a_{i}}_{\theta})$$

$$= \frac{1}{n} \sum_{i=1}^{n} \left(-(1-\epsilon) \sum_{j=1}^{N} \int_{l_{j-1}}^{l_{j}} \frac{\mathbb{I}(x \in \Delta_{E}^{i})}{\Delta} \log \frac{q^{s_{i},a_{i}}_{\theta}(\Delta_{j})}{\Delta} dx - \epsilon \sum_{j=1}^{N} \int_{l_{j-1}}^{l_{j}} \frac{p^{\mu}_{j}}{\Delta} \log \frac{q^{s_{i},a_{i}}_{\theta}(\Delta_{j})}{\Delta} dx \right)$$

$$= \frac{1}{n} \sum_{i=1}^{n} \left((1-\epsilon)(-\log q^{s_{i},a_{i}}_{\theta}(\Delta_{E}^{i})) + \epsilon \mathcal{H}(\widehat{\mu}^{s'_{i},\pi_{Z}(s'_{i})}, q^{s_{i},a_{i}}_{\theta}) \right) + (1-\epsilon)\Delta$$

$$\propto \frac{1}{n} \sum_{i=1}^{n} \left(-\log q^{s_{i},a_{i}}_{\theta}(\Delta_{E}^{i}) + \alpha \mathcal{H}(\widehat{\mu}^{s'_{i},\pi_{Z}(s'_{i})}, q^{s_{i},a_{i}}_{\theta}) \right), \text{ where } \alpha = \frac{\epsilon}{1-\epsilon} > 0$$

where recall that $\widehat{\mu}^{s_i',\pi_Z(s_i')} = \sum_{i=1}^N p_i^\mu(x) \mathbb{1}(x \in \Delta_i)/\Delta = \sum_{i=1}^N p_i^\mu/\Delta$ for conciseness and denote $q_{\theta}^{s_i,a_i} = \sum_{j=1}^N q_{\theta}^{s_i,a_i}(\Delta_j)/\Delta$. The cross-entropy $\mathcal{H}(\widehat{\mu}^{s_i',\pi_Z(s_i')},q_{\theta}^{s_i,a_i})$ is based on the discrete distribution when i=1,...,N. Δ_E^i represent the interval that $\mathbb{E}\left[\mathcal{R}(s_i,a_i)+\gamma Z_{\theta^*}^k\left(s_i',\pi_Z(s_i')\right)\right]$ falls into, i.e., $\mathbb{E}\left[\mathcal{R}(s_i,a_i)+\gamma Z_{\theta^*}^k\left(s_i',\pi_Z(s_i')\right)\right] \in \Delta_E^i$. \square

H. Proof of Proposition 3

Proposition 3 (Equivalence between the Mean-Related term in Decomposed Neural FZI and Neural FQI) In Eq. 3, assume the function class $\{Z_{\theta}: \theta \in \Theta\}$ is sufficiently large such that it contains the target $\{Y_i^k\}_{i=1}^n$, when $\Delta \to 0$, for all k, minimizing the mean-related term in Eq. 3 implies

$$P(Z_{\theta}^{k+1}(s,a) = \mathcal{T}^{\text{opt}}Q_{\theta^*}^k(s,a)) = 1, \quad \text{and} \quad \int_{-\infty}^{+\infty} \left| F_{q_{\theta}}(x) - F_{\delta_{\mathcal{T}^{\text{opt}}Q_{\theta^*}^k(s,a)}}(x) \right| dx = o(\Delta), \tag{28}$$

where $\mathcal{T}^{\text{opt}}Q_{\theta^*}^k(s,a)$ is the scalar-valued target in the k-th phase of Neural FQI, and $\delta_{\mathcal{T}^{\text{opt}}Q_{\theta^*}^k(s,a)}$ is the Dirac delta function defined on the scalar $\mathcal{T}^{\text{opt}}Q_{\theta^*}^k(s,a)$.

Proof. Limiting Case. Firstly, we define the distributional Bellman optimality operator \mathfrak{T}^{opt} as follows:

$$\mathfrak{T}^{\text{opt}}Z(s,a) \stackrel{D}{=} \mathcal{R}(s,a) + \gamma Z\left(S',a^*\right),\tag{29}$$

where $S' \sim P(\cdot \mid s, a)$ and $a^* = \underset{a'}{\operatorname{argmax}} \mathbb{E}\left[Z\left(S', a'\right)\right]$. If $\{Z_{\theta} : \theta \in \Theta\}$ is sufficiently large enough such that it contains $\mathfrak{T}^{\operatorname{opt}}Z_{\theta^*}\left(\{Y_i^k\}_{i=1}^n\right)$, then optimizing Neural FZI in Eq. 1 leads to $Z_{\theta}^{k+1} = \mathfrak{T}^{\operatorname{opt}}Z_{\theta^*}$.

Secondly, we apply the return density decomposition on the target histogram function $\widehat{p}^{s,a}(x)$. Consider the parameterized histogram density function h_{θ} and denote h_{θ}^{E}/Δ as the bin height in the bin Δ_{E} , under the KL divergence between the first histogram function $\mathbb{1}(x \in \Delta_{E})$ with $h_{\theta}(x)$, the objective function is simplified as

$$D_{\mathrm{KL}}(\mathbb{1}(x \in \Delta_E)/\Delta, h_{\theta}(x)) = -\int_{x \in \Delta_E} \frac{1}{\Delta} \log \frac{h_{\theta}^E}{\frac{\Delta}{\Delta}} dx = -\log h_{\theta}^E$$
(30)

Since $\{Z_{\theta}:\theta\in\Theta\}$ is sufficiently large enough that can represent the pdf of $\{Y_i^k\}_{i=1}^n$, it also implies that $\{Z_{\theta}:\theta\in\Theta\}$ can represent the mean-related term part in its pdf via the return density decomposition. The KL minimizer would be $\hat{h}_{\theta}=\mathbb{1}(x\in\Delta_E)/\Delta$ in expectation. Then, $\lim_{\Delta\to 0}\arg\min_{h_{\theta}}D_{\mathrm{KL}}(\mathbb{1}(x\in\Delta_E)/\Delta,h_{\theta}(x))=\delta_{\mathbb{E}[Z^{\mathrm{target}}(s,a)]}$, where $\delta_{\mathbb{E}[Z^{\mathrm{target}}(s,a)]}$ is a Dirac Delta function centered at $\mathbb{E}[Z^{\mathrm{target}}(s,a)]$ and can be viewed as a generalized probability density function. That being said, the limiting probability density function (pdf) converges to a Dirac delta function at $\mathbb{E}[Z^{\mathrm{target}}(s,a)]$. The limit behavior from a histogram function \widehat{p} to a continuous one for Z^{target} is guaranteed by Theorem 2, and this also applies from h_{θ} to Z_{θ} . In Neural FZI, we have $Z^{\mathrm{target}}=\mathfrak{T}^{\mathrm{opt}}Z_{\theta^*}$. Here, we use $Z^{k+1}_{\theta}(s,a)$ as the random variable whose cdf is the limiting distribution. According to the definition of the Dirac function, in the limiting case where $\Delta\to 0$, we attain that

$$\mathbb{P}(Z_{\theta}^{k+1}(s,a) = \mathbb{E}\left[\mathfrak{T}^{\text{opt}}Z_{\theta^*}^k(s,a)\right]) = 1.$$
(31)

This is because the pdf of the limiting return random variable $Z_{\theta}^{k+1}(s,a)$ is a Dirac delta function, which implies that the random variable takes this constant value with probability one. Due to the linearity of expectation in Lemma 4 of (Bellemare et al., 2017a), we have

$$\mathbb{E}\left[\mathfrak{T}^{\text{opt}}Z_{\theta^*}^k(s,a)\right] = \mathfrak{T}^{\text{opt}}\mathbb{E}\left[Z_{\theta^*}^k(s,a)\right] = \mathcal{T}^{\text{opt}}Q_{\theta^*}^k(s,a) \tag{32}$$

Finally, we obtain the convergence in probability one in the limiting case:

$$\mathbb{P}(Z_{\theta}^{k+1}(s,a) = \mathcal{T}^{\text{opt}}Q_{\theta^*}^k(s,a)) = 1 \quad \text{as } \Delta \to 0$$
(33)

Convergence in Distribution. The connection established above is in the limiting case. Alternatively, we can provide more formal proof by using the language of convergence in distribution. Here, we use $Z_{\theta,\Delta}^{k+1}$ to replace Z_{θ}^{k+1} to explicitly consider its asymptotic behavior. According to the fact that $\infty\{x\in\Delta_E\}/\Delta$ is the optimizer when minimizing the mean-related term in Eq. 3 given a fixed Δ , the convergence in distribution is:

$$\lim_{\Delta \to 0} \mathcal{D}(Z_{\theta,\Delta}^{k+1}) = \lim_{\Delta \to 0} \mathcal{D}(\mathbb{1}\{x \in \Delta_E\}/\Delta) = \mathcal{D}(\delta_{\mathcal{T}^{\text{opt}}Q_{\theta^*}(s,a)}), \tag{34}$$

where $\delta_{\mathcal{T}^{\mathrm{opt}}Q^k_{\theta^*}(s,a)}$ is the Dirac Delta function centered at $\mathcal{T}^{\mathrm{opt}}Q^k_{\theta^*}(s,a)$. $\mathcal{D}(\delta_{\mathcal{T}^{\mathrm{opt}}Q^k_{\theta^*}(s,a)})$ is the corresponding step function, where $\mathcal{D}(\delta_{\mathcal{T}^{\mathrm{opt}}Q^k_{\theta^*}(s,a)})(x)=1$ if $x\geq \mathcal{T}^{\mathrm{opt}}Q^k_{\theta^*}(s,a)$, and equals 0 otherwise. Note that the convergence in distribution in terms of the Dirac delta function implies that $\mathbb{P}(Z^{k+1}_{\theta}(s,a)=\mathcal{T}^{\mathrm{opt}}Q^k_{\theta^*}(s,a))=1$ as $\Delta\to 0$ in Eq 33.

Convergence Rate. In order to characterize how the difference varies when $\Delta \to 0$, we further define $\Delta_E = [l_e, l_{e+1})$ and we have:

$$\int_{-\infty}^{+\infty} \left| F_{q_{\theta}}(x) - F_{\delta_{\mathcal{T}^{\text{opt}}Q_{\theta^*}^k(s,a)}}(x) \right| dx = \frac{1}{2\Delta} \left(\left(\mathcal{T}^{\text{opt}}Q_{\theta^*}^k(s,a) - l_e \right)^2 + \left(l_{e+1} - \mathcal{T}^{\text{opt}}Q_{\theta^*}^k(s,a) \right)^2 \right) \\
= \frac{1}{2\Delta} (a^2 + (\Delta - a)^2) \\
\leq \Delta/2 \\
= o(\Delta),$$
(35)

where $\mathcal{T}^{\mathrm{opt}}Q_{\theta^*}^k(s,a) = \mathbb{E}\left[\mathfrak{T}^{\mathrm{opt}}Z_{\theta^*}^k(s,a)\right] \in \Delta_E$ and we denote $a = \mathcal{T}^{\mathrm{opt}}Q_{\theta^*}^k(s,a) - l_e$. The first equality holds as $q_{\theta}(x)$, the KL minimizer while minimizing the mean-related term, will follow a uniform distribution on Δ_E , i.e., $\widehat{q}_{\theta} = \mathbb{1}(x \in \Delta_E)/\Delta$. Thus, the integral of LHS would be the area of two centralized triangles accordingly. The inequality holds as the maximizer is obtained when $a = \Delta$ or 0. The result implies that the convergence rate in distribution difference is $o(\Delta)$.

I. Convergence Proof of DERPI in Theorem 1

I.1. Proof of Distribution-Entropy-Regularized Policy Evaluation in Lemma 1

Lemma 1(Distribution-Entropy-Regularized Policy Evaluation) Consider the distribution-entropy-regularized Bellman operator \mathcal{T}_d^{π} in Eq. 6 and assume $\mathcal{H}(\mu^{\mathbf{s}_t,\mathbf{a}_t},q_{\theta}^{\mathbf{s}_t,\mathbf{a}_t})$ is bounded for all $(\mathbf{s}_t,\mathbf{a}_t)\in\mathcal{S}\times\mathcal{A}$. Define $Q^{k+1}=\mathcal{T}_d^{\pi}Q^k$, then Q^{k+1} will converge to a *corrected* Q-value of π as $k\to\infty$ with the new objective function $J'(\pi)$ defined as

$$J'(\pi) = \sum_{t=0}^{T} \mathbb{E}_{(\mathbf{s}_{t}, \mathbf{a}_{t}) \sim \rho_{\pi}} \left[r\left(\mathbf{s}_{t}, \mathbf{a}_{t}\right) + \gamma f(\mathcal{H}\left(\mu^{\mathbf{s}_{t}, \mathbf{a}_{t}}, q_{\theta}^{\mathbf{s}_{t}, \mathbf{a}_{t}}\right)) \right].$$

Proof. Firstly, we plug in $V(\mathbf{s}_{t+1})$ into RHS of the iteration in Eq. 6, then we obtain

$$\mathcal{T}_{d}^{\pi}Q\left(\mathbf{s}_{t},\mathbf{a}_{t}\right) = r\left(\mathbf{s}_{t},\mathbf{a}_{t}\right) + \gamma \mathbb{E}_{\mathbf{s}_{t+1} \sim P\left(\cdot|\mathbf{s}_{t},\mathbf{a}_{t}\right)}\left[V\left(\mathbf{s}_{t+1}\right)\right] \\
= r\left(\mathbf{s}_{t},\mathbf{a}_{t}\right) + \gamma \mathbb{E}_{\mathbf{s}_{t+1} \sim P\left(\cdot|\mathbf{s}_{t},\mathbf{a}_{t}\right),\mathbf{a}_{t+1} \sim \pi}\left[f\left(\mathcal{H}(\mu^{\mathbf{s}_{t+1},\mathbf{a}_{t+1}},q_{\theta}^{\mathbf{s}_{t+1},\mathbf{a}_{t+1}})\right)\right] + \gamma \mathbb{E}_{\mathbf{s}_{t+1} \sim P\left(\cdot|\mathbf{s}_{t},\mathbf{a}_{t}\right),\mathbf{a}_{t+1} \sim \pi}\left[Q\left(\mathbf{s}_{t+1},\mathbf{a}_{t+1}\right)\right] \\
\triangleq r_{\pi}\left(\mathbf{s}_{t},\mathbf{a}_{t}\right) + \gamma \mathbb{E}_{\mathbf{s}_{t+1} \sim P\left(\cdot|\mathbf{s}_{t},\mathbf{a}_{t}\right),\mathbf{a}_{t+1} \sim \pi}\left[Q\left(\mathbf{s}_{t+1},\mathbf{a}_{t+1}\right)\right], \tag{36}$$

where $r_{\pi}\left(\mathbf{s}_{t}, \mathbf{a}_{t}\right) \triangleq r\left(\mathbf{s}_{t}, \mathbf{a}_{t}\right) + \gamma \mathbb{E}_{\mathbf{s}_{t+1} \sim P\left(\cdot \mid \mathbf{s}_{t}, \mathbf{a}_{t}\right), \mathbf{a}_{t+1} \sim \pi}\left[f\left(\mathcal{H}(\mu^{\mathbf{s}_{t+1}, \mathbf{a}_{t+1}}, q_{\theta}^{\mathbf{s}_{t+1}, \mathbf{a}_{t+1}})\right)\right]$ is the entropy augmented reward. Applying the standard convergence results for policy evaluation (Sutton & Barto, 2018), we can attain that this Bellman updating under \mathcal{T}_{d}^{π} is convergent under the assumption of $|\mathcal{A}| < \infty$ and bounded entropy augmented rewards r_{π} .

I.2. Policy Improvement with Proof

Lemma 2. (Distribution-Entropy-Regularized Policy Improvement) Let $\pi \in \Pi$ and a new policy π_{new} be updated via the policy improvement step in the policy optimization: $\pi_{new} = \arg\max_{\pi' \in \Pi} \mathbb{E}_{\mathbf{a}_t \sim \pi'} \left[Q^{\pi_{old}}(\mathbf{s}_t, \mathbf{a}_t) + f(\mathcal{H}(\mu^{\mathbf{s}_t, \mathbf{a}_t}, q_{\theta}^{\mathbf{s}_t, \mathbf{a}_t})) \right].$ Then $Q^{\pi_{new}}(\mathbf{s}_t, \mathbf{a}_t) \geq Q^{\pi_{old}}(\mathbf{s}_t, \mathbf{a}_t)$ for all $(\mathbf{s}_t, \mathbf{a}_t) \in \mathcal{S} \times \mathcal{A}$ with $|\mathcal{A}| < \infty$.

Proof. The policy improvement in Lemma 2 implies that $\mathbb{E}_{\mathbf{a}_t \sim \pi_{\text{new}}}[Q^{\pi_{\text{old}}}(\mathbf{s}_t, \mathbf{a}_t) + f(\mathcal{H}(\mu^{\mathbf{s}_t, \mathbf{a}_t}, q_{\theta}^{\mathbf{s}_t, \mathbf{a}_t}))] \geq \mathbb{E}_{\mathbf{a}_t \sim \pi_{\text{old}}}[Q^{\pi_{\text{old}}}(\mathbf{s}_t, \mathbf{a}_t) + f(\mathcal{H}(\mu^{\mathbf{s}_t, \mathbf{a}_t}, q_{\theta}^{\mathbf{s}_t, \mathbf{a}_t}))]$, we consider the Bellman equation via the distribution-entropy-regularized Bellman operator \mathcal{T}_{sd}^{π} :

$$Q^{\pi_{\text{old}}}\left(\mathbf{s}_{t}, \mathbf{a}_{t}\right) \triangleq r\left(\mathbf{s}_{t}, \mathbf{a}_{t}\right) + \gamma \mathbb{E}_{\mathbf{s}_{t+1} \sim P}\left[V^{\pi_{\text{old}}}\left(\mathbf{s}_{t+1}\right)\right]$$

$$= r\left(\mathbf{s}_{t}, \mathbf{a}_{t}\right) + \gamma \mathbb{E}_{\mathbf{s}_{t+1} \sim P}\left[\mathbb{E}_{\mathbf{a}_{t+1} \sim \pi_{\text{old}}}\left[f\left(\mathcal{H}(\mu^{\mathbf{s}_{t+1}, \mathbf{a}_{t+1}}, q_{\theta}^{\mathbf{s}_{t+1}, \mathbf{a}_{t+1}})\right) + Q^{\pi_{\text{old}}}\left(\mathbf{s}_{t+1}, \mathbf{a}_{t+1}\right)\right]\right]$$

$$\leq r\left(\mathbf{s}_{t}, \mathbf{a}_{t}\right) + \gamma \mathbb{E}_{\mathbf{s}_{t+1} \sim P}\left[\mathbb{E}_{\mathbf{a}_{t+1} \sim \pi_{\text{new}}}\left[f\left(\mathcal{H}(\mu^{\mathbf{s}_{t+1}, \mathbf{a}_{t+1}}, q_{\theta}^{\mathbf{s}_{t+1}, \mathbf{a}_{t+1}})\right) + Q^{\pi_{\text{old}}}\left(\mathbf{s}_{t+1}, \mathbf{a}_{t+1}\right)\right]\right]$$

$$= r\left(\mathbf{s}_{t}, \mathbf{a}_{t}\right) + \gamma \mathbb{E}_{\mathbf{s}_{t+1} \sim P, \mathbf{a}_{t+1} \sim \pi_{\text{new}}}\left[f\left(\mathcal{H}(\mu^{\mathbf{s}_{t+1}, \mathbf{a}_{t+1}}, q_{\theta}^{\mathbf{s}_{t+1}, \mathbf{a}_{t+1}})\right)\right] + \gamma \mathbb{E}_{\mathbf{s}_{t+1} \sim P, \mathbf{a}_{t+1} \sim \pi_{\text{new}}}\left[Q^{\pi_{\text{old}}}\left(\mathbf{s}_{t+1}, \mathbf{a}_{t+1}\right)\right]$$

$$= r_{\pi^{\text{new}}}\left(\mathbf{s}_{t}, \mathbf{a}_{t}\right) + \gamma \mathbb{E}_{\mathbf{s}_{t+1} \sim P, \mathbf{a}_{t+1} \sim \pi_{\text{new}}}\left[Q^{\pi_{\text{old}}}\left(\mathbf{s}_{t+1}, \mathbf{a}_{t+1}\right)\right]$$

$$\vdots$$

$$\leq Q^{\pi_{\text{new}}}\left(\mathbf{s}_{t+1}, \mathbf{a}_{t+1}\right),$$
(37)

where $Q^{\pi_{\text{old}}}$ ($\mathbf{s}_{t+1}, \mathbf{a}_{t+1}$) indicates that the future actions are taking following π_{old} , given \mathbf{s}_{s+t} and \mathbf{a}_{t+1} . We have repeated expanded $Q^{\pi_{\text{old}}}$ on the RHS by applying the distribution-entropy-regularized distributional Bellman operator. Each following step will then incorporate the actions following the new policy. Convergence to $Q^{\pi_{\text{new}}}$ follows from Lemma 1.

I.3. Proof of DERPI in Theorem 1

Theorem 1 (Distribution-Entropy-Regularized Policy Iteration) Repeatedly applying distribution-entropy-regularized policy evaluation in Eq. 6 and the policy improvement, the policy converges to an optimal policy π^* such that $Q^{\pi^*}(\mathbf{s}_t, \mathbf{a}_t) \geq Q^{\pi}(\mathbf{s}_t, \mathbf{a}_t)$ for all $\pi \in \Pi$.

Proof. The proof is similar to soft policy iteration (Haarnoja et al., 2018a). For completeness, we provide the proof here. By Lemma 2, as the number of iteration increases, the sequence Q^{π_i} at i-th iteration is monotonically increasing. Since we assume the uncertainty-aware entropy is bounded, the Q^{π} is thus bounded as the rewards are bounded. Hence, the sequence will converge to some π^* . Further, we prove that π^* is in fact optimal. At the convergence point, for all $\pi \in \Pi$, it must be case that:

$$\mathbb{E}_{\mathbf{a}_{t} \sim \pi^{*}} \left[Q^{\pi_{\text{old}}} \left(\mathbf{s}_{t}, \mathbf{a}_{t} \right) \right] \geq \mathbb{E}_{\mathbf{a}_{t} \sim \pi} \left[Q^{\pi_{\text{old}}} \left(\mathbf{s}_{t}, \mathbf{a}_{t} \right) \right].$$

According to the proof in Lemma 2, we can attain $Q^{\pi^*}(\mathbf{s}_t, \mathbf{a}_t) > Q^{\pi}(\mathbf{s}_t, \mathbf{a}_t)$ for $(\mathbf{s}_t, \mathbf{a}_t)$. That is to say, the "corrected" value function of any other policy in Π is lower than the converged policy, indicating that π^* is optimal.

I.4. Discussion about DERPI with Varying q_{θ}

In the tabular setting, we have shown that the convergence of DERPI holds given a fixed q_{θ} . The primary goal for us to derive this convergence result is to demonstrate the uncertainty-aware regularized exploration promoted by the decomposed regularization from (categorical) distributional loss. If we hope to develop a further algorithm in the function approximation, we need to consider how to interplay a parameterized Q function, policy, and q. For example, we may leverage separate neural network works for each component. Alternatively, we can use one single neural network to represent the whole return distribution (q_{θ}) and then take the expectation to evaluate the Q function. This extension indeed motivates the design of our DERAC algorithm, which we provide in Appendix J for interested readers.

J. DERAC Algorithm: Interpolating AC and Distributional AC

J.1. Algorithm Design

Motivation. The convergence guarantee of DERPI given a fixed q_{θ} in Section 5.1 provides sufficient insights to understand the uncertainty-aware regularized exploration. To further substantiate the validity of introducing the decomposed entropy

into the actor-critic with the general function approximation, we extend DERPI into a practical algorithm with favorable interpretability. Unlike SAC, which introduces another value function network, we only parameterize the return distribution $q_{\theta}(s_t, a_t)$ and the policy $\pi_{\phi}(a_t|s_t)$, where we use $\mathbb{E}\left[q_{\theta}\right]$ to represent the Q function without parameterizing it again. Remarkably, the resulting *Distribution-Entropy-Regularized Actor-Critic (DERAC)* algorithm can interpolate expectation-based AC and distributional AC.

Optimize the critic q_{θ} . The new value function $\hat{J}_q(\theta)$ is originally trained to minimize the squared residual error of Eq. 6. We show that $\hat{J}_q(\theta)$ can be simplified as:

$$\hat{J}_{q}(\theta) \propto (1 - \lambda) \mathbb{E}_{s,a} \left[\left(\mathcal{T}^{\pi} \mathbb{E} \left[q_{\theta^{*}}(s, a) \right] - \mathbb{E} \left[q_{\theta}(s, a) \right] \right)^{2} \right] + \lambda \mathbb{E}_{s,a} \left[\mathcal{H}(\mu^{s,a}, q_{\theta}^{s,a}) \right], \tag{38}$$

where we use a particular increasing function $f(\mathcal{H}) = (\tau \mathcal{H})^{\frac{1}{2}}/\gamma$ and $\lambda = \frac{\tau}{1+\tau} \in [0,1], \tau \geq 0$ is the hyperparameter that controls the uncertainty-aware regularization effect. The proof is given in Appendix J.2. Interestingly, when we leverage the whole target density function $\hat{p}^{s,a}$ to approximate the true return distribution of $\mu^{s,a}$, the objective function in Eq. 38 can be viewed as an exact interpolation of loss functions between expectation-based AC (the first term) and categorical distributional AC loss (the second term) (Ma et al., 2020). In our implementation, for the target $\mathcal{T}^{\pi}\mathbb{E}\left[q_{\theta^*}(s,a)\right]$, we use the target return distribution neural network q_{θ^*} to stabilize the training, which is consistent with the Neural FZI framework analyzed in Section 4.1.

Optimize the policy π_{ϕ} . We optimize π_{ϕ} in the policy optimization based on the Q-function, and therefore the new objective function $\hat{J}_{\pi}(\phi)$ can be expressed as:

$$\hat{J}_{\pi}(\phi) = \mathbb{E}_{s,a \sim \pi_{\phi}} \left[\mathbb{E} \left[q_{\theta}(s,a) \right] + \left(\tau \mathcal{H}(\mu^{s,a}, q_{\theta}^{s,a}) \right)^{\frac{1}{2}} / \gamma \right]$$
(39)

The complete DERAC algorithm is presented in Algorithm 2 of Appendix J.3.

Remark on DERAC and Its Difference from Categorical Distributional AC. The careful neural architecture design and selection of the function f endow the loss function of DERAC with interpretability. However, the DERAC algorithm is not our main focus; rather, it primarily serves to substantiate the efficacy of the uncertainty-aware regularized exploration in distributional RL within an actor-critic framework rather than to achieve superior real-world performance. In contrast to Categorical Distributional AC, which depends entirely on distributional learning in policy optimization, DERAC interpolates between expectation-based and distributional learning. In Section J.4, we empirically demonstrate that this interpolation form can be more suitable in specific environments than distributional AC, helping to *mitigate the excessive exploration* in fully distributional learning.

J.2. Proof of Interpolation Form of $\hat{J}_q(\theta)$

In SAC (Haarnoja et al., 2018a) (Section 4.2), it introduces another parameterized state value function to approximate the soft value in the function approximation setting. Instead, we do not intend to do so but directly use a single Q network to be optimized, which allows the interpolation form of our algorithm. In particular, we directly evaluate the least squared loss between the current Q estimates and the target ones for the critic loss. With a particular form of $\hat{f}_{\pi}(\mathcal{H})$, the removal of the interaction term, and the replacement of Q_{θ} with $\mathbb{E}\left[q_{\theta}\right]$, we can derive the interpolation form of $\hat{J}_{q}(\theta)$ according to the following formula:

$$\hat{J}_{q}(\theta) = \mathbb{E}_{s,a} \left[\left(\mathcal{T}_{d}^{\pi} Q_{\theta^{*}}(s,a) - Q_{\theta}(s,a) \right)^{2} \right] \\
= \mathbb{E}_{s,a} \left[\left(\mathcal{T}^{\pi} Q_{\theta^{*}}(s,a) - Q_{\theta}(s,a) + \gamma (\tau^{1/2} \mathcal{H}^{1/2}(\mu^{s,a}, q_{\theta}^{s,a})/\gamma) \right)^{2} \right] \\
= \mathbb{E}_{s,a} \left[\left(\mathcal{T}^{\pi} \mathbb{E} \left[q_{\theta^{*}}(s,a) \right] - \mathbb{E} \left[q_{\theta}(s,a) \right] \right)^{2} \right] + \tau \mathbb{E}_{s,a} \left[\mathcal{H}(\mu^{s,a}, q_{\theta}^{s,a}) \right] \\
+ \mathbb{E}_{s,a} \left[\left(\mathcal{T}^{\pi} \mathbb{E} \left[q_{\theta^{*}}(s,a) \right] - \mathbb{E} \left[q_{\theta}(s,a) \right] \right) \mathcal{H}(\mu^{s,a}, q_{\theta}^{s,a}) \right] \\
\approx \mathbb{E}_{s,a} \left[\left(\mathcal{T}^{\pi} \mathbb{E} \left[q_{\theta^{*}}(s,a) \right] - \mathbb{E} \left[q_{\theta}(s,a) \right] \right)^{2} \right] + \tau \mathbb{E}_{s,a} \left[\mathcal{H}(\mu^{s,a}, q_{\theta}^{s,a}) \right] \\
\propto (1 - \lambda) \mathbb{E}_{s,a} \left[\left(\mathcal{T}^{\pi} \mathbb{E} \left[q_{\theta^{*}}(s,a) \right] - \mathbb{E} \left[q_{\theta}(s,a) \right] \right)^{2} \right] + \lambda \mathbb{E}_{s,a} \left[\mathcal{H}(\mu^{s,a}, q_{\theta}^{s,a}) \right],$$

where the second equation is based on the definition of Distribution-Entropy-Regularized Bellman Operator \mathcal{T}_d^{π} in Eq. 6 and let $f(\mathcal{H}) = (\tau \mathcal{H})^{1/2}/\gamma$. The interaction term $\mathbb{E}_{s,a}\left[(\mathcal{T}^{\pi}\mathbb{E}\left[q_{\theta^*}(s,a)\right] - \mathbb{E}\left[q_{\theta}(s,a)\right])\mathcal{H}(\mu^{s,a},q_{\theta}^{s,a})\right]$ equal zero in the last equation is rooted in Lemma 1 in (Shi et al., 2022). Although Lemma 1 considers the A/B testing with the offline dataset, it demonstrates that the estimation equation between the Bellman error and any function $\varphi\left(\mathbf{s}_t,\mathbf{a}_t\right)$ equals zero under mild conditions, such as the consistency assumption. Strictly speaking, we heuristically extend the conclusion in Lemma 1 of (Shi et al., 2022) to the simplification of our critic loss, where we let $\varphi\left(\mathbf{s}_t,\mathbf{a}_t\right) = \mathcal{H}(\mu^{\mathbf{s}_t,\mathbf{a}_t},q_{\theta^{s_t,\mathbf{a}_t}}^{\mathbf{s}_t,\mathbf{a}_t})$. Consequently, we can approximately remove the interaction term as $\mathbb{E}_{s,a}\left[(\mathcal{T}^{\pi}\mathbb{E}\left[q_{\theta^*}(s,a)\right] - \mathbb{E}\left[q_{\theta}(s,a)\right])\mathcal{H}(\mu^{s,a},q_{\theta}^{s_t,\mathbf{a}_t})\right] = 0$. We set $\lambda = \frac{\tau}{1+\tau} \in [0,1]$. Another simplification is that we directly use $\mathbb{E}\left[q_{\theta}\right]$ to replace Q_{θ} rather than to maintain both two networks q_{θ} and Q_{θ} with different parameters θ . This strategy simplifies our implementation and contributes to deriving the final interpolation form in $\hat{J}_q(\theta)$.

J.3. DERAC Algorithm

We provide a detailed algorithm description of DERAC algorithm in Algorithm 2.

Algorithm 2 Distribution-Entropy-Regularized Actor Critic (DERAC) Algorithm

```
1: Initialize two value networks q_{\theta}, q_{\theta^*}, soft updating rates \lambda_{\pi}, \lambda_q, \tau_q \in [0, 1], and policy network \pi_{\phi}.
      for each iteration do
          for each environment step do
 4:
              a_t \sim \pi_\phi(a_t|s_t).
 5:
               s_{t+1} \sim p(s_{t+1}|s_t, a_t).
              \mathcal{D} \leftarrow \mathcal{D} \cup \{(s_t, a_t, r(s_t, a_t), s_{t+1})\}
 6:
 7:
          end for
          for each gradient step do
 8:
              \theta \leftarrow \theta - \lambda_q \nabla_{\theta} \hat{J}_q(\theta)
 9:
10:
               \phi \leftarrow \phi + \lambda_{\pi} \nabla_{\phi} J_{\pi}(\phi).
               \theta^* \leftarrow \tau_a \theta + (1 - \tau_a) \theta^*
11:
          end for
13:
      end for
```

J.4. Experiments on DERAC: Mitigating the Excessive Exploration

Baseline Algorithms.

- AC: The implementation of AC is directly from the standard SAC algorithm (Haarnoja et al., 2018a) without using the entropy regularization.
- DAC (C51). Based on the original implementation of AC, we employ the C51 loss in the critic loss. Thus, the performance difference between DAC (C51) and AC is merely the leverage of distributional loss.
- DERAC: Our proposed algorithm in Section J is based on the implementation of AC, which uses an interpolated critic loss. The experiments on DERAC are used to validate the convergence analysis in Section J and highlight the potential

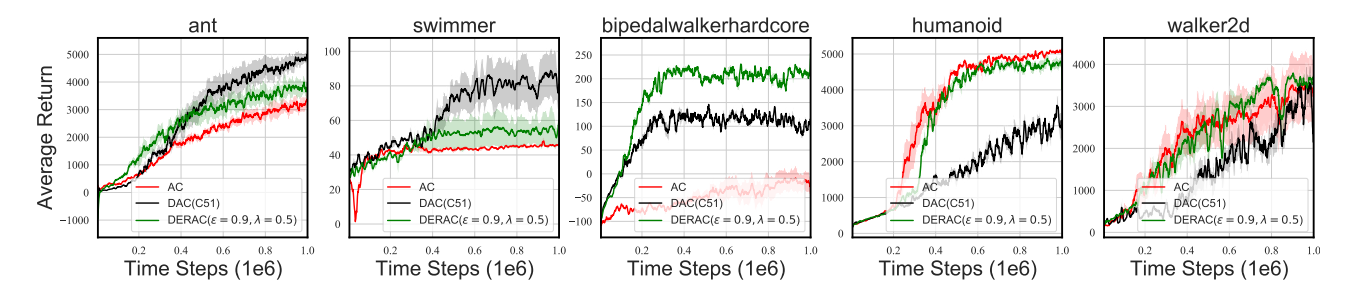


Figure 6: Learning curves of DERAC over five seeds on MuJoCo. No vanilla entropy regularization is used in AC or DAC. **Group 1**: Ant, Swimmer and Bipedalwalkerhardcore, where DAC (C51) outperforms AC. **Group 2**: Humanoid and Walker2d, where AC outperforms DAC (C51).

performance improvement of an interpolated algorithm in mitigating the over-exploration for an entire distribution RL algorithm.

We examine the interpolation performance of the proposed DERAC algorithm in continuous control environments to substantiate the uncertain-aware regularized exploration in actor-critic algorithms. Figure 6 suggests that DERAC (green) converges and tends to "interpolate" between the expectation-based AC and distributional AC denoted by DAC (C51), substantiating the theoretical convergence of the tabular DERPI algorithm in Theorem 1. We highlight that *the primary purpose of introducing DERAC is to interpret the benefits of CDRL from the perspective of uncertain-aware regularized exploration rather than to pursue empirical superiority*. In **Group 1**, it is essential to note that DERAC achieves superior performance over both AC and DAC (C51) on bipedalwalkerhardcore, verifying that the interpolation has extra advantages. We posit that the interpolation nature of DERAC mitigates the over-exploration when adopting the purely categorical distributional learning in C51, as a pure CDRL algorithm may put too much emphasis on the uncertainty-aware exploration, i.e., all weight on the regularization term in Entropy-regularized Neural FQI in Eq. 3. In **Group 2** where DAC is inferior to AC, it exhibits that DERAC performs similarly to or slightly excels at AC. These results demonstrate that DERAC is more robust and can even surpass DAC (C51) by potentially mitigating the over-exploration of pure distributional RL. Unlike fully distributional RL, which puts more weight on uncertainty-aware regularized exploration, DERAC offers a more optimal balance between exploration and exploitation, potentially resulting in better performance in certain environments. We also provide a sensitivity analysis of DERAC regarding λ in Appendix J.5.

J.5. Sensitivity Analysis of DERAC

Figure 7 shows that DERAC with different λ in Eq. 38 may behave differently in different environments. In general, DERAC with different ε and λ perform similarly to DERAC, with an interpolation nature between AC and DAC (C51). Notably, DERAC with different ε and λ still surpasses both AC and DAC (C51) in bidedalwalkerhardcore, demonstrating the robust superiority of the DERAC algorithm.

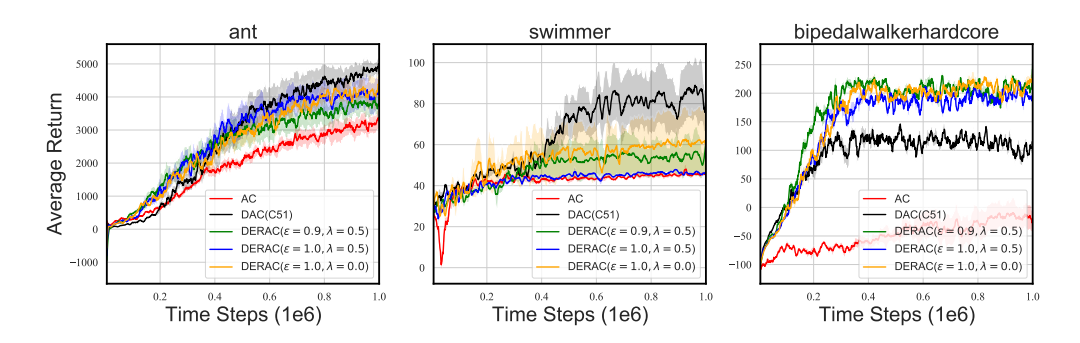


Figure 7: Learning curves of DERAC algorithms across different λ and ε on three MuJoCo environments over 5 seeds.

K. Implementation Details

K.1. Baselines Algorithms

Algorithms in Section 6.1.

- DQN (Mnih et al., 2015) and C51 (Bellemare et al., 2017a)
- $\mathcal{H}(\mu, q_{\theta})(\varepsilon = X)$: a variant of C51 algorithm, where we replace the original target histogram function $\widehat{p}^{s,a}$ with the induced $\widehat{\mu}^{s,a}$ for each (s,a) pair in the update. By varying $\varepsilon = X$, $\mathcal{H}(\mu, q_{\theta})$ relies on the distributional loss to different extents in the RL learning. For examples, when $\varepsilon = 1$, $\mathcal{H}(\mu, q_{\theta})(\varepsilon = X)$ degenerates to the vanilla C51 algorithm. On the contrary, decreasing ε in $\mathcal{H}(\mu, q_{\theta})$ will reduce the leverage of knowledge from the distributional loss, leading to performance degradation in a distributional learning context.

Algorithms in Section 6.2.

- AC: This implementation is the same as AC in Section J.4.
- AC+VE: This is exactly the standard SAC algorithm.
- AC+UE: This implementation is also the same as DAC (C51) in Section J.4, where we use a distributional critic loss in the AC algorithm.
- AC+UE+VE: Based on the SAC algorithm, i.e., AC+VE, we additionally use the distribution objective in C51 as the critic loss.

K.2. Replacing ϵ with the ratio ε for Visualization

The substitution of ϵ with ε is for convenience in the implementation. As Proposition 1 elucidates, the return density decomposition requires that ϵ exceed certain thresholds to ensure the resultant decomposed $\widehat{\mu}^{s,a}$ qualifies as a valid density function. In practice, pinpointing this lower boundary for ϵ in each iteration to regulate its range could be prohibitively time-intensive. A more pragmatic approach involves redistributing the mass from the bin that contains the expectation to other bins in specified ratios, thereby introducing the corresponding ratio term ε . By varying ε from 0 to 1, it invariably meets the validity condition outlined in Proposition 1, thereby streamlining the process for conducting ablation studies concerning $\widehat{\mu}^{s,a}$ as demonstrated in Figure 3.

To delineate the relationship between the ratio ε and the coefficient ϵ in constructing $\widehat{\mu}^{s,a}$, after some calculations we establish their equivalence as follows:

$$\varepsilon = \frac{p_E - (1 - \epsilon)}{p_E \epsilon},\tag{41}$$

where p_E represents the weighting assigned to the bin Δ_E as specified in Proposition 1. The resulting $\varepsilon \in [0,1]$ has a monotonically increasing relationship with ϵ . In addition, $\epsilon = 1$ implies $\varepsilon = 1$. These properties facilitate the visualization without undermining our conclusion.

Decomposition Details. By varying ε , we can evaluate ϵ via the transformation equation in Eq. 41, which guarantees the validity of return density decomposition. Next, under different ϵ , we compute the induced histogram density $\hat{\mu}^{s,a}$ via the return density decomposition in Eq. 2:

$$\widehat{\mu}^{s,a}(x) = \widehat{p}^{s,a}(x \notin \Delta_E)/\epsilon + \widehat{p}^{s,a}(x \in \Delta_E)\varepsilon, \tag{42}$$

where combines Eq. 2 and Eq. 41. Importantly, by summing all the probabilities of p_i^{μ} in μ , we have:

$$\sum_{i=1}^{n} p_i^{\mu} = \frac{1 - p_E}{\epsilon} + \frac{p_E - (1 - \epsilon)}{\epsilon} = 1.$$
 (43)

This substantiates the validity of our decomposition by using ε instead of ϵ for visualization. Next, we replace $\widehat{p}^{s,a}$ with $\widehat{\mu}^{s,a}$ in C51 or the critic loss in Distributional AC (C51) as the decomposed algorithm $\mathcal{H}(\mu, q_{\theta})$ and compare the performance of all considered algorithms. Please refer to the code in the implementation for more details.

K.3. Hyper-parameters and Network structure

Our implementation is adapted from the popular RLKit platform. For Distributional SAC with C51, we use 51 atoms similar to the C51 (Bellemare et al., 2017a). For distributional SAC with quantile regression, instead of using fixed quantiles in QR-DQN, we leverage the quantile fraction generation based on IQN (Dabney et al., 2018a) that uniformly samples quantile fractions in order to approximate the full quantile function. In particular, we fix the number of quantile fractions as N and keep them in ascending order. Besides, we adapt the sampling as $\tau_0 = 0$, $\tau_i = e_i / \sum_{i=0}^{N-1} e_i$, where $\epsilon_i \in U[0,1], i=1,...,N$. We adopt the same hyper-parameters, which are listed in Table 1 and network structure as in the original distributional SAC paper (Ma et al., 2020).

L. Experiments Results

L.1. Uncertainty-aware Regularization Effect by Varying ϵ in Actor Critic

We study the uncertainty-aware regularization effect from being categorical distributional in the actor-critic framework, where we decompose the C51 critic loss in Distributional SAC (DSAC) according to Eq. 2. We denote the decomposed

Table 1: Hyper-parameters Sheet.

Hyperparameter	Value
Shared	
Policy network learning rate	3e-4
(Quantile) Value network learning rate	3e-4
Optimization	Adam
Discount factor	0.99
Target smoothing	5e-3
Batch size	256
Replay buffer size	1e6
Minimum steps before training	1e4
DSAC with C51	
Number of Atoms (N)	51
DSAC with IQN	
Number of quantile fractions (N)	32
Quantile fraction embedding size	64
Huber regression threshold	1

Hyperparameter	Temperature Parameter β	Max episode lenght
Walker2d-v2	0.2	1000
Swimmer-v2	0.2	1000
Reacher-v2	0.2	1000
Ant-v2	0.2	1000
HalfCheetah-v2	0.2	1000
Humanoid-v2	0.05	1000
HumanoidStandup-v2	0.05	1000
BipedalWalkerHardcore-v2	0.002	2000

DSAC (C51) with different ε as $\mathcal{H}(\mu,q_\theta)(\varepsilon=0.9/0.5/0.1)$.. As suggested in Figure 8, the performance of $\mathcal{H}(\mu,q_\theta)$ tends to vary from the vanilla DSAC (C51) to SAC with the decreasing of ε on four MuJoCo environments. In some environments, the difference of $\mathcal{H}(\mu,q_\theta)$ across various ε may not be pronounced between DSAC (C51) and SAC. We hypothesize that the algorithm performance is not sufficiently sensitive when ε changes within this restricted range. Although $\varepsilon \in (0,1)$ is designed to guarantee a valid density decomposition, it does not guarantee that ε in Eq. 2 can flexibly vary from 0 to 1. It is worth noting that our return density decomposition is valid only when $\varepsilon \geq 1 - p_E$ as shown in Proposition 1, and therefore ε can not strictly go to 0, where $\mathcal{H}(\mu,q_\theta)$ would degenerate to SAC ideally. Therefore, compared with the ablation study in Figure 3, the trend varying from DSAC to SAC in Figure 8 by decreasing ε may not be as pronounced as that in value-based RL evaluated on Atari games. One crucial reason behind is that the actor-critic architecture is generally perceived to be more prone to instability compared to value-based learning in RL. As outlined in (Fujimoto et al., 2018), this instability stems from the policy updates, which likely introduces additional bias or variance from the critic learning process.

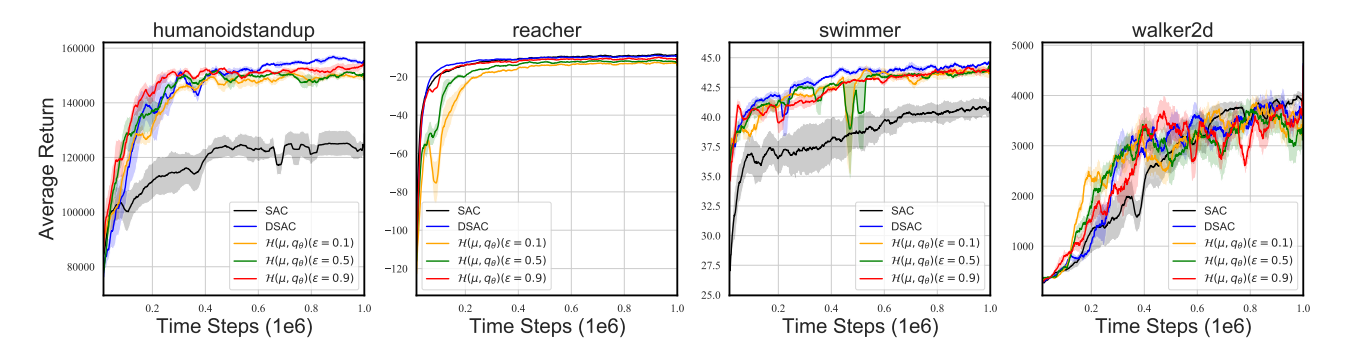


Figure 8: Learning curves of DSAC (C51) with the return distribution decomposition $\mathcal{H}(\mu, q_{\theta})$ under different ε .

L.2. Mutual Impacts on DSAC (C51)

In Figure 9, we present results over DSAC (C51) on the same eight MuJoCo environments as DSAC (IQN) in Figure 4. Figures 9 showcases that the simultaneous leverage of uncertainty-aware and vanilla entropy regularization could render either a mutual improvement or a potential interference. For examples, it turns out that AC+UE+VE outperforms both AC+VE (SAC) and AC+UE (DAC) on humanoidstandup. By contrast, it suggests performance degradation in half of environments when the two regularizations are employed together, such as ant and swimmer, where AC+UE+VE is significantly inferior to AC+UE or AC+VE.

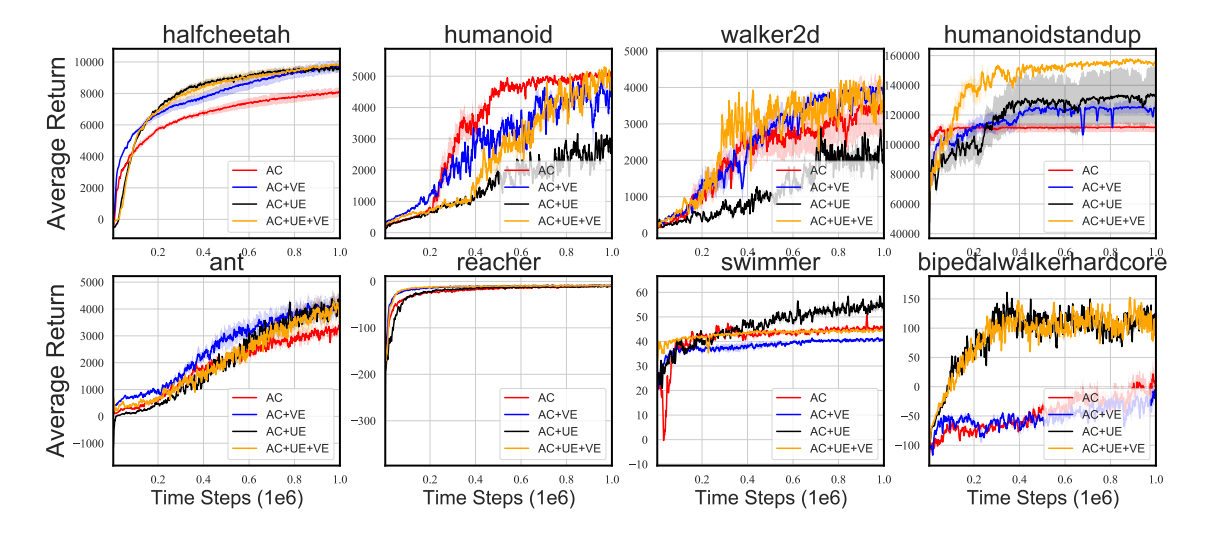


Figure 9: Learning curves of *AC*, *AC*+*VE* (SAC), *AC*+*UE* (DAC) and AC+UE+VE (DSAC) over five seeds across seven MuJoCo environments where distributional RL part is based on C51. (Walker 2d, Humanoidstandup, Reacher, and Bipedalwalkerhardcore): Mutual Improvement. (Halfcheetah, Humanoid, Ant, and Swimmer): Potential Interference.

L.3. Ablation Study across Different Bin Sizes (Number of Atoms)

To further demonstrate our regularization effect based on the return density decomposition, we conducted an additional ablation study by varying the number of bins/atoms (equivalent to adjusting the bin sizes) of both C51 and our decompose algorithm $\mathcal{H}(\mu, q_{\theta})$. Consistent with the tendency shown in Figure 3 in Section 6.1, Figure 10 also suggests that decreasing ε implies that $\mathcal{H}(\mu, q_{\theta})$ degrades from C51 with the same bin size to DQN. Another interesting observation is that, as shown in Breakout (the first row in Figure 10), increasing the number of atoms (reducing the bin size) restricts the range of ε for a valid return density decomposition in Proposition 1. Consequently, a small number of atoms or a large bin size can allow a broader variation of $\mathcal{H}(\mu, q_{\theta})$ from C51 to DQN, facilitating the demonstration of our regularization effect empirically.

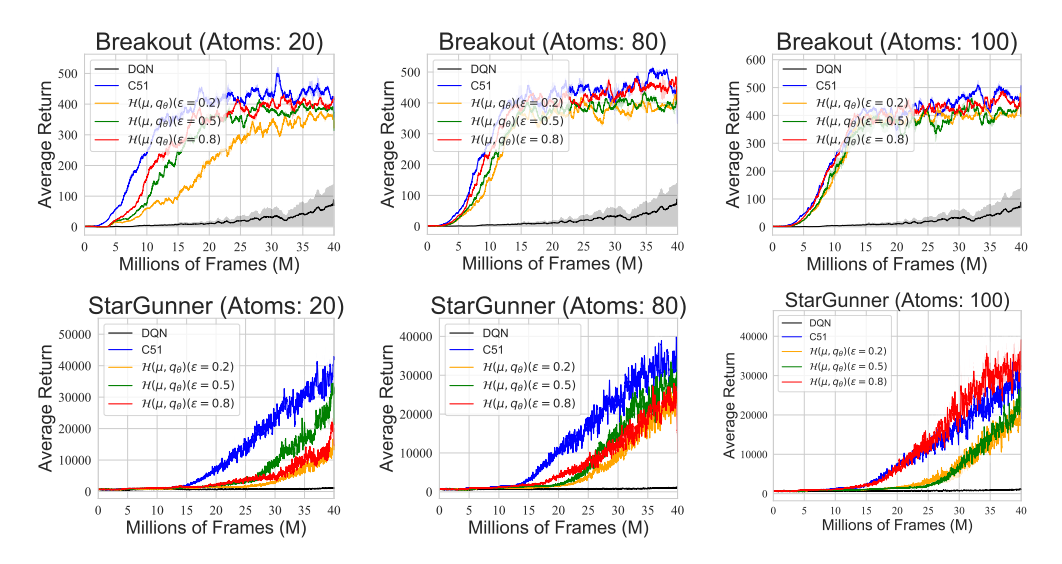


Figure 10: Learning curves of value-based CDRL, i.e., C51 algorithm, and the decomposed algorithm $\mathcal{H}(\mu, q_{\theta})$ across different numbers of atoms (various bin sizes) on two Atari games. Results are averaged over three seeds, and the shade represents the standard deviation.

M. Discussion on Decomposing Quantile-based Distributional Loss

In order to extend our analysis and conclusion to broader distributional RL algorithm classes, we need to discuss another commonly-used algorithm based on quantile regression loss (Dabney et al., 2018b;a). Although it may be possible to discuss both categorical and quantile representation based on the particle representation (Definition 5.13 in (Bellemare et al., 2023)), committing either fixed atoms in categorical representation or fixed quantiles in quantile representation can simplify the algorithm analysis. In this section, we discuss how to decompose the quantile-based distributional loss in quantile regression distributional RL.

Quantile-based Distributional Loss. In each phase of Neural FZI, we know that the return distribution, parameterized by quantiles, is fixed. This, therefore, leads to a *composite quantile loss* (Zou & Yuan, 2008), which is initially developed to capture the full conditional distribution of the response variable by predicting or estimating its multiple quantiles:

$$\ell_{\text{quantile}} = \frac{1}{N} \sum_{i=1}^{N} \mathbb{E}_{y \sim P_Y} \left[\rho_{\tau_i} \left(y - Z_{\theta}^{\tau_i} \right) \right], \tag{44}$$

where ρ_{τ_i} is the quantile (pinball) loss defined by $\rho_{\tau_i}(u) = u\left(\tau_i - \mathbb{1}_{\{u < 0\}}\right)$, $\forall u \in \mathbb{R}$. We use P_Y to denote the fixed target return distribution. In quantile-based distributional RL, we can directly sample y from the quantile function F_Y^{-1} of the fixed target return given that both the current and target return distributions are parameterized by the quantiles. $Z_{\theta}^{\tau_i}$ represents the estimated τ_i -quantile value of the current return distribution. Alternatively, ρ_{τ_i} can be the quantile Huber loss (Huber, 1992), a smooth version of vanilla quantile loss at zero, by additionally introducing a hyper-parameter κ . We thus denote the quantile Huber loss as $\rho_{\tau_i}^{\kappa}$, which is defined as:

$$\rho_{\tau_i}^{\kappa}(u) = \left| \tau_i - \mathbb{1}_{\{u < 0\}} \right| \frac{\mathcal{L}_{\kappa}(u)}{\kappa},\tag{45}$$

where

$$\mathcal{L}_{\kappa}(u) = \begin{cases} \frac{1}{2}u^2, & \text{if } |u| \le \kappa \\ \kappa \left(|u| - \frac{1}{2}\kappa\right), & \text{otherwise} \end{cases}$$
 (46)

As $\kappa \to 0$, it is easy to show that the quantile Huber loss reverts to the vanilla quantile loss. To simplify the notation, we consider the inner-level loss for a fixed y:

$$L_{\text{quantile}} = \frac{1}{N} \sum_{i=1}^{N} \rho_{\tau_i} (y - Z_{\theta}^{\tau_i}).$$
 (47)

Quantile Representation and Asymptotic Mean-Preserving Property. The normal representation and categorical representation with the categorical projection $\Pi_{\mathcal{C}}$ in Eq. 9 could satisfy the mean-preserving property (Section 4.3 in (Rowland et al., 2019)), as seen in (5.18) in Section 5.4 for normal representation (Bellemare et al., 2023) and in Lemma 4.8 for categorical representation in (Rowland et al., 2019). By contrast, quantile distributional dynamic programming is generally not mean-preserving (Lemma 4.8 in (Rowland et al., 2019)), as the quantiles are non-linear functionals of distribution. However, we show that the quantile representation has an asymptotic mean-preserving property as the mean of quantiles is asymptotically equivalent to the expectation of the considered distribution when the number of quantiles tends to infinity. Particularly, assume that we have N evenly spaced quantiles $\{\frac{i}{N+1}\}_{i=1}^{N}$, we approximate the expectation by the mean of all quantiles values defined by

$$\frac{1}{N} \sum_{i=1}^{N} F^{-1}(\frac{i}{N+1}),\tag{48}$$

Consequently, given a random variable X with its quantile function F^{-1} , we have the following property of quantile function:

$$\lim_{N \to +\infty} \frac{1}{N} \sum_{i=1}^{N} F^{-1}(\frac{i}{N+1}) = \int_{0}^{1} F^{-1}(\tau) d\tau = \int_{-\infty}^{+\infty} x dF(x) = \mathbb{E}[X], \tag{49}$$

where the first equation results from the relationship between the limit of Riemann Sum and its integral, and the second equation holds by changing the variable $\tau = F(x)$. Note that this asymptotic regime is similar to that in our histogram

function analysis for CDRL, where $\Delta \to 0 \iff N \to +\infty$. According to this equivalence regarding the mean quantiles and the expectation of a random variable, we consider the two decomposition ways as follows.

Decomposition Method 1. We denote $\bar{Z} = \frac{1}{N} \sum_{i=1}^{N} Z_{\theta}^{\tau_i}$ as the mean of the quantiles for the *current* return. Consequently, we have a straightforward composition as follows:

$$\rho_{\tau_i}^{\kappa}\left(y - Z_{\theta}^{\tau_i}\right) = \rho_{\tau_i}^{\kappa}\left(\left(y - \bar{Z}\right) + \left(\bar{Z} - Z_{\theta}^{\tau_i}\right)\right) = \rho_{\tau_i}^{\kappa}\left(y - \bar{Z}\right) + \delta_{\tau},\tag{50}$$

where

$$\delta_{\tau} = \rho_{\tau_i}^{\kappa} \left((y - \bar{Z}) + (\bar{Z} - Z_{\theta}^{\tau_i}) \right) - \rho_{\tau_i}^{\kappa} (y - \bar{Z}). \tag{51}$$

Therefore, we have the decomposed composite quantile loss as

$$L_{\text{quantile}} = \underbrace{\frac{1}{N} \sum_{i=1}^{N} \rho_{\tau_{i}}^{\kappa}(y - \bar{Z})}_{\text{Mean-Related Term}} + \underbrace{\frac{1}{N} \sum_{i=1}^{N} \delta_{\tau}}_{\text{Residual Term}}.$$
(52)

The first term is a mean-related one, which we will elaborate on later, while the induced δ_{τ} in the residual term is aimed at capturing the distribution information beyond only the expectation. Particularly, minimizing $\rho_{\tau_i}^{\kappa} \left((y - \bar{Z}) + (\bar{Z} - Z_{\theta}^{\tau_i}) \right)$ in δ_{τ} will push the deviations $\bar{Z} - Z_{\theta}^{\tau_i}$ from the current return estimator to capture the deviations from the target return distribution of $y - \bar{Z}$. This regularization term contributes to preserving the richness of the quantile representation for distributional information, especially the dispersion, from the return.

In terms of the mean-related term, let us consider the approximation. As the quantile Huber loss is typically used in quantile-based distributional RL, when κ is large, the mean-related term can be simplified as

$$\frac{1}{N} \sum_{i=1}^{N} \rho_{\tau_i}^{\kappa}(y - \bar{Z}) \approx \frac{1}{N} \sum_{i=1}^{N} \left| \tau_i - \mathbb{1}_{\{y - \bar{Z} < 0\}} \right| \frac{1}{2} (y - \bar{Z})^2 \approx \frac{1}{4} (y - \bar{Z})^2, \tag{53}$$

where the first approximation holds because $\mathcal{L}_{\kappa}(u) = \frac{1}{2}u^2$ with high probability. The second approximation holds because $|\tau_i - \mathbbm{1}_{\{y = \bar{Z} < 0\}}| \frac{1}{2}(y - \bar{Z})^2$ is just the quantile value scaled version of least squared loss. Since \bar{Z} is the expectation of all estimated quantiles, it can be approximately symmetric to $\mathbb{E}[Y]$. Suppose $P(y - \bar{Z} < 0) = P(y - \bar{Z} \ge 0) = \frac{1}{2}$, we have

$$\mathbb{E}\left[\left|\tau_{i} - \mathbb{1}_{\{y - \bar{Z} < 0\}}\right|\right] = \frac{1}{2}\left(\left|\tau_{i} - 1\right| + \tau_{i}\right) = \frac{1}{2}.$$
(54)

Therefore, this approximation in the mean-related term holds, as shown in Eq. 53. This implies that the mean quantile estimator $Z_{\hat{\theta}} = \arg\min_{\bar{Z}} \mathbb{E}_{y \sim P_Y} \left[y - \frac{1}{N} \sum_{i=1}^N Z_{\theta}^{\tau_i} \right]^2$ captures the expectation of the target return distribution from $y \sim P_Y$. Recap the asymptotic equivalence between the expected quantiles and the true expectation of a random variable in Eq. 49, the limiting estimator of $Z_{\hat{\theta}}$ by minimizing the mean-related term in $\ell_{quantile}$ satisfies:

$$\mathbb{E}[Y] = \frac{1}{N} \sum_{i=1}^{N} Z_{\hat{\theta}}^{\tau_i} \to \mathbb{E}[Z_{\hat{\theta}}] \quad \text{as} \quad N \to +\infty.$$
 (55)

This implies that the learned expected return $\mathbb{E}\left[Z_{\hat{\theta}}\right]$ is asymptotically mean-preserving when minimizing the mean-related term in the quantile-based distributional loss.

In summary, the first decomposition method decomposes the quantile-base distributional loss into the mean-related and residual terms. After a mild approximation, the mean-related term can be simplified as a least-squared loss equipped with an expected quantiles estimator. Combining the equivalence regarding the limiting behavior of the expected quantiles, the mean-related term is thus approximately equivalent to the standard least-squared loss used in classical RL, thus asymptotically satisfying the mean-preserving property. Moreover, the residual term is able to capture the return distribution information beyond its expectation. In the context of uncertain-aware regularized exploration in our paper, the residual term plays a similar role to the cross-entropy-based regularization derived in Proposition 2 of CDRL.

Decomposition Method 2. Another decomposition method can directly follow the return density decomposition proposed in Eq. 2, but we apply the decomposition on the quantile function $F^{-1}(\tau)$ for $\tau \in [0, 1]$. We expect that this decomposition

Intrinsic Benefits of Categorical Distributional Loss: Uncertainty-aware Regularized Exploration in Reinforcement Learning

also leads to two parts, where the first part can involve the quantile defined on the bin $\Delta_{\bar{\tau}}$ that contains the expected quantiles $\bar{F}^{-1} = \sum_{i=1}^N F^{-1}(\tau_i)$, and the second term relates to the distribution part. However, this detailed decomposition is largely beyond the scope of this paper, and it takes more effort to think about it carefully. We leave this decomposition regarding the quantile-based distributional loss as future work.